ENGINEERING OF BIOMATERIALS

INŻYNIERIA BIOMATERIAŁÓW

JOURNAL OF POLISH SOCIETY FOR BIOMATERIALS AND FACULTY OF MATERIALS SCIENCE AND CERAMICS AGH-UST

CZASOPISMO POLSKIEGO STOWARZYSZENIA BIOMATERIAŁÓW I WYDZIAŁU INŻYNIERII MATERIAŁOWEJ I CERAMIKI AGH

Number 157
Numer 157
Volume XXIII
Rok XXIII

OCTOBER 2020
PAŹDZIERNIK 2020

ISSN 1429-7248

PUBLISHER:
WYDAWCA:

Polish Society for Biomaterials in Krakow
Polskie Stowarzyszenie Biomateriałów w Krakowie

ADDRESS OF EDITORIAL OFFICE:
ADRES REDAKCJI:

AGH-UST
30/A3, Mickiewicz Av.
30-059 Krakow, Poland
Akademia Górniczo-Hutnicza
al. Mickiewicza 30/A-3
30-059 Kraków

Issue: 250 copies
Nakład: 250 egz.

Scientific Publishing House AKAPIT
Wydawnictwo Naukowe AKAPIT
e-mail: wn@akapit.krakow.pl

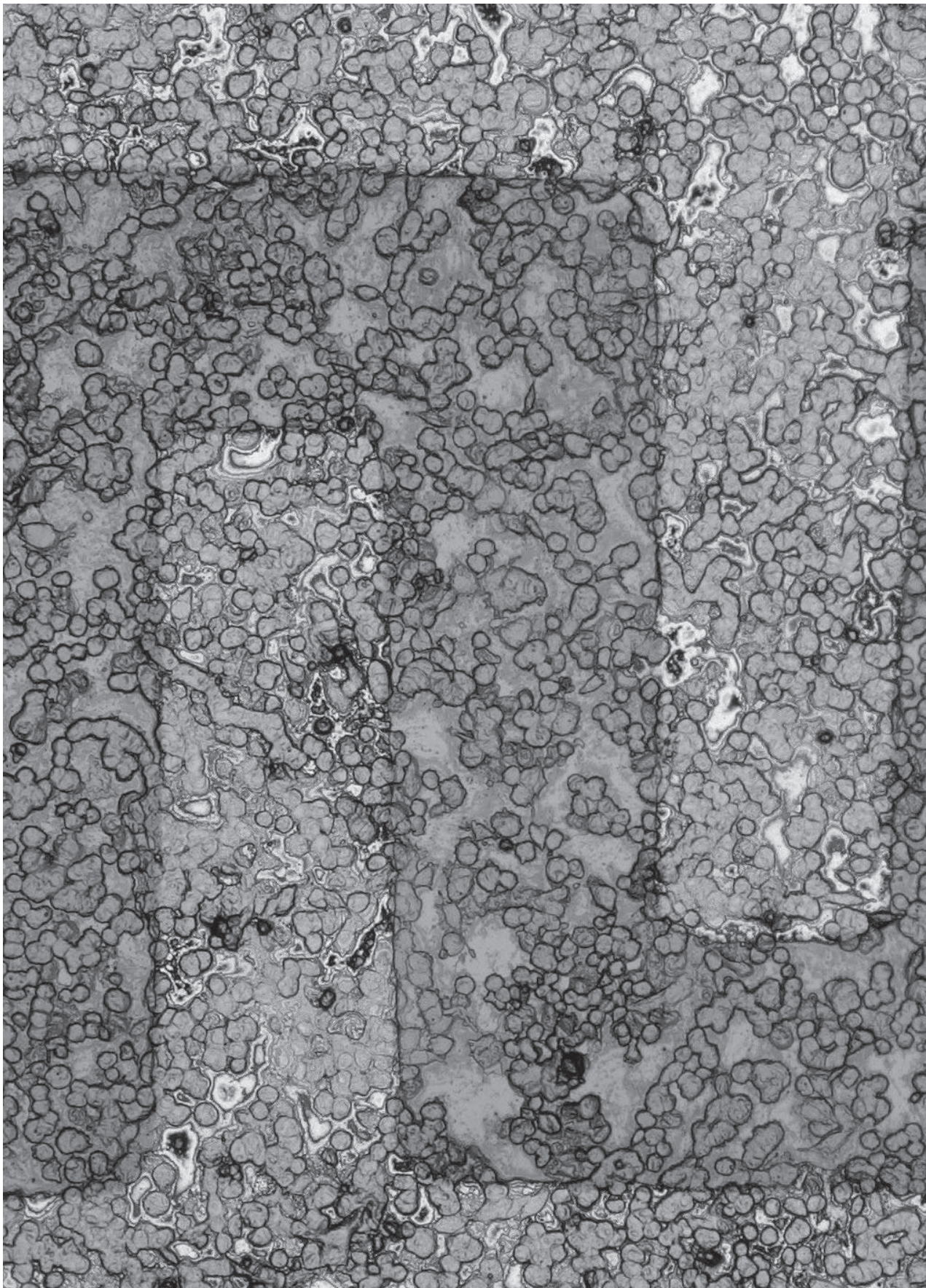

ENGINEERING OF BIOMATERIALS

EDITORIAL BOARD
KOMITET REDAKCYJNY

INTERNATIONAL EDITORIAL BOARD
MIĘDZYNARODOWY KOMITET REDAKCYJNY

ENGINEERING OF BIOMATERIALS

Wskazówki dla autorów

1. Prace do opublikowania w kwartalniku „Engineering of Biomaterials / Inżynieria Biomateriałów" przyjmowane będą wyłącznie w języku angielskim.
2. Wszystkie nadsyłane artykuły są recenzowane.
3. Materiały do druku prosimy przysyłać za pomocą systemu online (www.biomaterials.pl).
4. Struktura artykułu:
• TYTUŁ • Autorzy i instytucje • Streszczenie (200-250 słów) • Słowa kluczowe (4-6) • Wprowadzenie • Materiały i metody • Wyniki i dyskusja • Wnioski • Podziękowania • Piśmiennictwo
5. Autorzy przesyłają pełną wersję artykułu, łącznie z ilustracjami, tabelami, podpisami i literaturą w jednym pliku. Artykuł w tej formie przesyłany jest do recenzentów. Dodatkowo autorzy proszeni są o przesłanie materiałów ilustracyjnych (rysunki, schematy, fotografie, wykresy) w oddzielnych plikach (format np. .jpg, .gif., .tiff, .bmp). Rozdzielczość rysunków min. 300 dpi. Wszystkie rysunki i wykresy powinny być czarno-białe lub w odcieniach szarości i ponumerowane cyframi arabskimi. W tekście należy umieścić odnośniki do rysunków i tabel. W przypadku artykułów dwujęzycznych w tabelach i na wykresach należy umieścić opisy polskie i angielskie.
6. Na końcu artykułu należy podać wykaz piśmiennictwa w kolejności cytowania w tekście i kolejno ponumerowany.
7. Redakcja zastrzega sobie prawo wprowadzenia do opracowań autorskich zmian terminologicznych, poprawek redakcyjnych, stylistycznych, w celu dostosowania artykułu do norm przyjętych w naszym czasopiśmie. Zmiany i uzupełnienia merytoryczne będą dokonywane w uzgodnieniu z autorem.
8. Opinia lub uwagi recenzentów będą przekazywane Autorowi do ustosunkowania się. Nie dostarczenie poprawionego artykułu w terminie oznacza rezygnację Autora z publikacji pracy w naszym czasopiśmie.
9. Za publikację artykułów redakcja nie płaci honorarium autorskiego.
10. Adres redakcji:

Czasopismo
„Engineering of Biomaterials / Inżynieria Biomateriałów"
Akademia Górniczo-Hutnicza im. St. Staszica
Wydział Inżynierii Materiałowej i Ceramiki
al. Mickiewicza 30/A-3, 30-059 Kraków
tel. (48) 12 617 44 48, 12 617 25 61
tel./fax: (48) 12 617 45 41
e-mail: epamula@agh.edu.pl, kabe@agh.edu.pl

Szczegółowe informacje dotyczące przygotowania manuskryptu oraz procedury recenzowania dostępne są na stronie internetowej czasopisma:
www.biomaterials.pl

Warunki prenumeraty

Zamówienie na prenumeratę prosimy przesyłać na adres:
mgr inż. Augustyn Powroźnik
apowroz@agh.edu.pl, tel/fax: (48) 12 617 45 41
Cena pojedynczego numeru wynosi 20 PLN
Konto: Polskie Stowarzyszenie Biomateriałów
30-059 Kraków, al. Mickiewicza 30/A-3
ING Bank Śląski S.A. O/Kraków
nr rachunku 63 1050 1445 1000 0012 0085 6001

Prenumerata obejmuje 4 numery regularne i nie obejmuje numeru specjalnego (materiały konferencyjne).

Instructions for authors

1. Papers for publication in quarterly journal „Engineering of Biomaterials / Inżynieria Biomateriałów" should be written in English.
2. All articles are reviewed.
3. Manuscripts should be submitted to editorial office through online submission system (www.biomaterials.pl).
4. A manuscript should be organized in the following order:
• TITLE • Authors and affiliations • Abstract (200-250 words) • Keywords (4-6) • Introduction • Materials and Methods • Results and Discussions • Conclusions • Acknowledgements • References
5. All illustrations, figures, tables, graphs etc. preferably in black and white or grey scale should be additionally sent as separate electronic files (format .jpg, .gif., .tiff, .bmp). High-resolution figures are required for publication, at least 300 dpi. All figures must be numbered in the order in which they appear in the paper and captioned below. They should be referenced in the text. The captions of all figures should be submitted on a separate sheet.
6. References should be listed at the end of the article. Number the references consecutively in the order in which they are first mentioned in the text.
7. The Editors reserve the right to improve manuscripts on grammar and style and to modify the manuscripts to fit in with the style of the journal. If extensive alterations are required, the manuscript will be returned to the authors for revision.
8. Opinion or notes of reviewers will be transferred to the author. If the corrected article will not be supplied on time, it means that the author has resigned from publication of work in our journal.
9. Editorial does not pay author honorarium for publication of article.
10. Address of editorial office:

Journal
„Engineering of Biomaterials / Inżynieria Biomateriałów"
AGH University of Science and Technology
Faculty of Materials Science and Ceramics
30/A-3, Mickiewicz Av., 30-059 Krakow, Poland
tel. (48) 12) 617 44 48, 12 617 25 61
tel./fax: (48) 12 617 45 41
e-mail: epamula@agh.edu.pl, kabe@agh.edu.pl

Detailed information concerning manuscript preparation and review process are available at the journal's website:
www.biomaterials.pl

Subscription terms

Contact:
MSc Augustyn Powroźnik,
e-mail: apowroz@agh.edu.pl
Subscription rates:
Cost of one number: 20 PLN
Payment should be made to:
Polish Society for Biomaterials
30/A3, Mickiewicz Av.
30-059 Krakow, Poland
ING Bank Slaski S.A.
account no. 63 1050 1445 1000 0012 0085 6001

Subscription includes 4 issues and does not include special issue (conference materials).

STUDIA PODYPLOMOWE

Biomateriały – Materiały dla Medycyny

2020/2021

Organizator: Akademia Górniczo-Hutnicza im. Stanisława Staszica w Krakowie Wydział Inżynierii Materiałowej i Ceramiki Katedra Biomateriałów i Kompozytów **Kierownik:** prof. dr hab. inż. Elżbieta Pamuła **Sekretarz:** dr inż. Małgorzata Krok-Borkowicz	**Adres:** 30-059 Kraków, Al. Mickiewicza 30 Pawilon A3, p. 208, 210 lub 501 tel. 12 617 44 48, 12 617 23 38, fax. 12 617 33 71 email: epamula@agh.edu.pl; krok@agh.edu.pl https://www.agh.edu.pl/ksztalcenie/oferta-ksztalcenia/studia-podyplomowe-kursy-doksztalcajace-i-szkolenia/biomaterialy-materialy-dla-medycyny/

Charakterystyka:
Tematyka prezentowana w trakcie zajęć obejmuje przegląd wszystkich grup materiałów dla zastosowań medycznych: metalicznych, ceramicznych, polimerowych, węglowych i kompozytowych. Słuchacze zapoznają się z metodami projektowania i wytwarzania biomateriałów a następnie możliwościami analizy ich właściwości mechanicznych, właściwości fizykochemicznych (laboratoria z metod badań: elektronowa mikroskopia skaningowa, mikroskopia sił atomowych, spektroskopia w podczerwieni, badania energii powierzchniowej i zwilżalności) i właściwości biologicznych (badania: *in vitro* i *in vivo*). Omawiane są regulacje prawne i aspekty etyczne związane z badaniami na zwierzętach i badaniami klinicznymi (norma EU ISO 10993). Słuchacze zapoznają się z najnowszymi osiągnięciami w zakresie nowoczesnych nośników leków, medycyny regeneracyjnej i inżynierii tkankowej.

Sylwetka absolwenta:
Studia adresowane są do absolwentów uczelni technicznych (inżynieria materiałowa, technologia chemiczna), przyrodniczych (chemia, biologia, biotechnologia) a także medycznych, stomatologicznych, farmaceutycznych i weterynaryjnych, pragnących zdobyć, poszerzyć i ugruntować wiedzę z zakresu inżynierii biomateriałów i nowoczesnych materiałów dla medycyny. Słuchacze zdobywają i/lub pogłębiają wiedzę z zakresu inżynierii biomateriałów. Po zakończeniu studiów wykazują się znajomością budowy, właściwości i sposobu otrzymywania materiałów przeznaczonych dla medycyny. Potrafią analizować wyniki badań i przekładać je na zachowanie się biomateriału w warunkach żywego organizmu. Ponadto słuchacze wprowadzani są w zagadnienia dotyczące wymagań normowych, etycznych i prawnych niezbędnych do wprowadzenia nowego materiału na rynek. Ukończenie studiów pozwala na nabycie umiejętności przygotowywania wniosków do Komisji Etycznych i doboru metod badawczych w zakresie analizy biozgodności materiałów.

Zasady naboru:
Termin zgłoszeń: od 20.09.2020 do 20.10.2020 (liczba miejsc ograniczona - decyduje kolejność zgłoszeń)
Wymagane dokumenty: dyplom ukończenia szkoły wyższej
Osoby przyjmujące zgłoszenia:
prof. dr hab. inż. Elżbieta Pamuła (pawilon A3, p. 208, tel. 12 617 44 48, e-mail: epamula@agh.edu.pl)
dr inż. Małgorzata Krok-Borkowicz (pawilon A3, p. 210, tel. 12 617 23 38, e-mail: krok@agh.edu.pl)

Czas trwania: 2 semestry (od XI 2020 r. do VI 2021 r.) 8 zjazdów (soboty-niedziele) 1 raz w miesiącu	**Opłaty:** 2 600 zł (za dwa semestry)

30th Biomaterials in Medicine and Veterinary Medicine

Anniversary Conference

14 – 17 October 2021 Rytro, Poland

SAVE THE DATE

14-17

OCTOBER

2021

www.biomat.agh.edu.pl

REGISTER

AND

SUBMIT

AN ABSTRACT

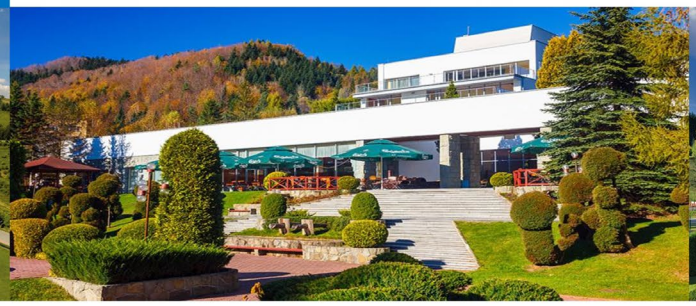

ENGINEERING OF BIOMATERIALS

SPIS TREŚCI
CONTENTS

Wersja papierowa czasopisma „Engineering of Biomaterials / Inżynieria Biomateriałów" jest jego wersją pierwotną
Printed version of „Engineering of Biomaterials / Inżynieria Biomateriałów" is a primary version of the journal

ASSESSMENT OF MECHANICAL STRENGTH AND CORROSION RESISTANCE AT VARIABLE pH OF ORTHODONTIC WIRES

Joanna Augustyn-Nadzieja[1*], Agnieszka Szczotok[2]

[1] AGH University of Science and Technology, Faculty of Metals Engineering and Industrial Computer Science, Department of Physical and Powder Metallurgy, Mickiewicza Av. 30, 30-059 Krakow, Poland
[2] Silesian University of Technology, Faculty of Materials Engineering, Department of Advanced Materials and Technologies, Krasinskiego Str. 8, 40-019 Katowice, Poland
*e-mail: jap@agh.edu.pl

Abstract

Orthodontic wires are components of fixed appliances used to perform the necessary tooth movements in the course of the orthodontic treatment. A variety of materials e.g. metals, alloys, polymers and composites are used to produce orthodontic wires. This study examined the mechanical strength and cracks resistance of three different types of wires, i.e. made of: austenitic steel grade AISI 303, NiTi alloy and Tiβ alloy. Corrosion processes are regarded to have a harmful effect on the properties of orthodontic wires, such as their strength, biocompatibility and aesthetic appearance. In this study, we investigated the corrosive behaviour of the wires in the artificial saliva solutions with varied pH simulating the natural oral cavity environment. It was demonstrated that the orthodontic rectangular wires made of austenitic steel grade AISI 303 exhibited the highest tensile strength. The NiTi alloy wires exhibited the best plastic properties of all the examined samples. In the case of electrochemical tests (changes in corrosion potential over a period of 24 h), the wire made of austenitic steel and the NiTi alloy wire reached a stable level of the stationary potential in the acidic environment. For the wires made of Tiβ, the highest stationary potential was observed in the alkaline environment. Additionally, the Tiβ alloy wire revealed the broadest passivation area in the specified potential scope.

Keywords: *tensile test, orthodontic wires, austenitic steel, nitinol (NiTi), Tiβ, corrosion resistance*

[Engineering of Biomaterials 157 (2020) 2-9]

doi:10.34821/eng.biomat.157.2020.2-9

Introduction

Malocclusion may result from abnormalities in the structure and position of the jaw bones in relation to each other or from a disturbed arrangement of the dental arches. It may be a hereditary or acquired condition, leading to distorted speech, difficulty breathing or eating. In such cases, orthodontic treatment is helpful for patients because of both health and aesthetics [1-3].

The orthodontic treatment is carried out for adolescents and adults, and concerns primarily in correcting crowded, rotated, buried or prominent front teeth. The group of 6000 children in Polish elementary schools was screened for dental caries by Wrigley Polska Company in 2014. The studies revealed that up to 60% of pupils required orthodontic treatment [4]. According to [5], 60% of people in Poland have a malocclusion.

The application of alloys with elastic memory dates back to the 1970s when Andreasen began their promotion in orthodontics [6]. In modern stomatology, the wires are made of alloys characterized by a one- and two-directional effect of elastic memory and superelasticity [7-9]. The most popular and frequently used orthodontic wires are arches made of the NiTi (Nitinol) alloy, the beta-type titanium alloy (Tiβ) and stainless austenitic steel [10-12]. The developments in nickel-titanium (NiTi) wire technology lowered the popularity of stainless steel wires for initial alignment. However, stainless steel archwires are still used by a small proportion of orthodontists [13]. During the treatment, the choice of the orthodontic wire is not random. The selection of the metallic material (wire) is dictated by a good corrosion resistance in the environment of the oral cavity, where the electrolyte is mostly constituted by the saliva and the food products consumed by the patient [14-16].

Nickel compounds have been well established as carcinogenic but their underlying mechanisms are still not fully understood. Yet not all nickel compounds are equally carcinogenic, because their carcinogenic potency is directly related to their ability to enter cells [17]. Nickel is the most common metal to cause contact dermatitis in orthodontics but nickel-titanium alloys and stainless steel are widely used in orthodontic appliances. Nickel-titanium alloys may contain nickel in excess of 50%, which can potentially result in an allergic reaction. Stainless steel has a lower nickel content (8%) and because the nickel is bound in a crystal lattice it is not available to react [18]. The good corrosion resistance of the NiTi alloy is mainly provided by titanium oxides which form a coherent passive layer on the surface of the material [14,19,20]. Austenitic corrosion-resistant steels were the first metals implanted in the human body. The content of austenite and ferrite-forming elements should be selected taking into account their impact so that the austenite is thermodynamically stable [21]. The presence of chromium in the amount above 13% ensures a positive corrosion potential and good corrosion resistance in oxidizing environments. Additionally, chromium reduces the passivation current density and increases the resistance to pitting corrosion [15,16,22]. As the nickel content increases, the resistance to stress corrosion cracking increases [23]. The operation time of austenitic steel should not exceed 2 years, due to the stress corrosion, material destruction and toxic elements penetrating the body tissue [22]. A very popular and commonly available biomedical material is titanium due to its high corrosion resistance, also in physiological fluids. The Tiβ alloy is mono-phase, therefore it possesses better anticorrosive and tribological properties than the dual-phase alloy α+β [15,16,24].

Materials and Methods

In the research three types of orthodontic wires were investigated: a rectangular wire made of austenitic steel grade AISI 303, with the dimensions 0.48x0.63x167 mm (FIG. 1a), a wire made of Nitinol alloy (NiTi), Ø = 0.5 mm in diameter and l = 160 mm long (FIG. 1b) and a rectangular wire made of beta-type titanium alloy (Tiβ), with the dimensions 0.4x0.55x160 mm (FIG. 1c).

The rectangular wire made of austenitic steel (FIG. 1a) is suitable for big malocclusions, where a high force is required and it is mostly used in the first stage of the orthodontic treatment. Rectangular arches made of austenitic steel are characterized by the best resistance to the operation of the tooth's movement forces [2,25]. They are applied for a sagittal shift of the teeth in the side segment, arrangement of the canines in I canine class, arrangement of the incisors in the proper angulation, correction of the median line. In the contraction phase, they are used to arrange the canine teeth in the proper sagittal position. The NiTi alloy orthodontic wire (FIG. 1b) is used at the beginning of the orthodontic treatment to level the position of the brackets in the horizontal and vertical plane [2,25]. Additionally, it prevents rotation and is responsible for the position of the molar teeth. Such an arch also makes sure that the molar teeth and the canine teeth assume the proper direction of levelling. The Tiβ orthodontic wire (FIG. 1c) has a smooth surface. It is used both in the course and the contraction of the treatment to provide: sagittal shifts of the teeth in the side segment, "artistic" arrangement of the incisors, correction of the incisors, correction of the median line, levelling of rotation [2,25]. The Tiβ wires are usually used in the case of patients allergic to nickel. The chemical compositions of the examined wires used in orthodontic treatment are presented in TABLE 1.

The strength tests of the analyzed materials were performed according to the PN-EN 10002-1 standard [27]. They were carried out with the use of a Zwick/Roell Z250 tester equipped with tensometric sensors and electronic extensometers. With the use of the Test Expert V5 program, it was possible to precisely steer the power feed and to record all the parameters in the scope of a static tensile test with the assumed deformation-stress cyclogram. In the case of the presented investigation results, a tensometric sensor with the scope of the measured force of up to 10 kN and an electronic extensometer with a varying measurement base (80 mm) was applied. The test parameters were the 50 N initial force and the 5 mm/min movement speed of the traverse. For each examined wire, three static tensile tests were performed and the results presented as averaged values.

The scanning electron microscope HITACHI S-3500N was used to examine the wires surface after the pull tests.

The oral cavity environment is highly moist and subjected to the temperature and pH changes depending on beverage and food consumed, thus it favours dental materials degradation [28]. The electrochemical tests were carried out in a physiological solution of artificial saliva, whose chemical composition is given in TABLE 2 [29]. Saliva plays a key role in lubrication, mastication, taste perception, prevention of oral infection and dental caries. Saliva is one of the most important factors in preventing dental caries, too [30]. The tests were performed to determine the effect of a varying pH of the artificial saliva solution on the corrosion resistance of the examined wires made of austenitic steel, alloy NiTi and alloy Tiβ. TABLE 2 shows the chemical composition of the artificial saliva treated as an environment with a physiological pH of 7.4. Additions of HCl (for pH = 4.0) and NaOH (for pH = 8.0) were applied to obtain various pH values of the artificial saliva.

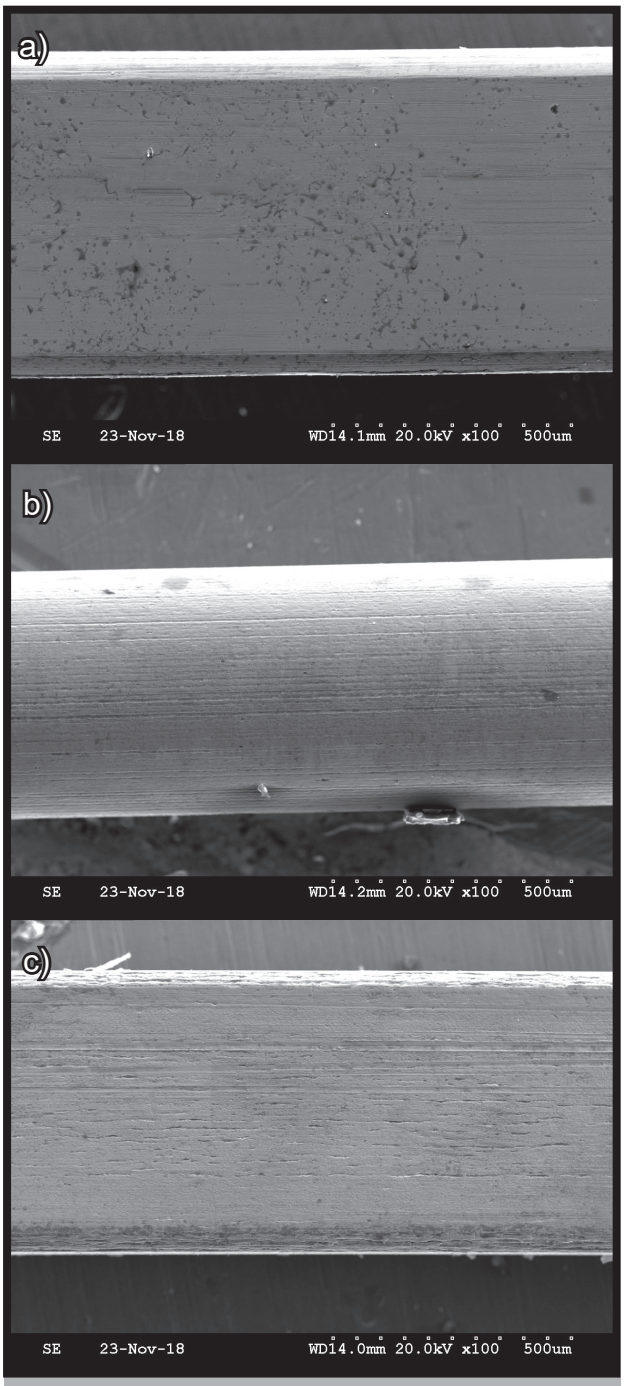

FIG. 1. SEM images of the surface morphology of orthodontic wires made of AISI 303 austenitic steel (a), NiTi alloy (b), Tiβ alloy (c).

TABLE 1. Chemical composition of orthodontic wires made of austenitic steel AISI 303 grade (a) [19], NiTi (Nitinol) (b) [18,19] and Tiβ alloy (c) [25,26].

a) Chemical composition, % mass.				
Cr	**Ni**	**Mn**	**Co**	**Fe**
18	9	2	0.75	rest
b) Chemical composition, % mass.				
Ni	**Ti**			
55.82	rest			
c) Chemical composition, % mass.				
Zr	**Mo**	**Sn**	**Ti**	
4-8	8-12	2-5	rest	

The examinations of the corrosion resistance of the orthodontic wires were conducted by means of stationary potential meters OCP – Keithley 2000 Multimeter and potentiostat Autolab PGSTAT302N. The electrochemical tests for each of the tested wires, and for each of the pH values lasted 24 h.

The electrochemical tests on a global scale were performed by means of a standard electrolytic vessel with 3 electrodes (FIG. 2) [24]. The vessel contained a working electrode (the examined sample of an orthodontic arch made of: austenitic steel grade AISI 303 or alloy NiTi or Tiβ), a platinum counter-electrode and a reference electrode (chlorosilver electrode).

The tests were carried out in the artificial saliva solution with free access to air. The measurements were made in a water bath with a constant temperature of 37°C where the electrochemical vessel was placed. By means of the potentiostat, the accelerated tests were performed using electroless techniques (a stationary Open Circuit Potential for spontaneous processes) and direct current techniques (Linear Sweep Voltammetry potentiodynamic polarization with a constant potential change rate 1 mV/s).

TABLE 2. Chemical composition of a simulated saliva solution per 1 litre of distilled water [29].

MAS - Mayer Artificial Saliva Solution	The content of component [g], calculated per 1 litre of distilled water
NaCl	0.7
KCl	1.2
$NaHCO_3$	1.5
Na_2HPO_4	0.26
KSCN	0.3
$Na_2S \cdot 9H_2O$	0.005
Urea	1.0
pH of the solution	**7.4**

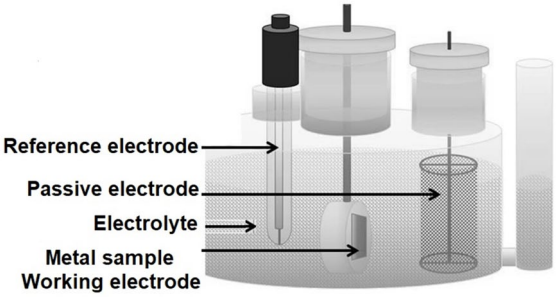

FIG. 2. Electrochemical vessel for research on a global scale [24].

Results and Discussion

The purpose of the static tensile tests was to determine the basic mechanical properties of the examined orthodontic wires, i.e. the Young modulus (E), the yield point $R_{p0,2}$, the tensile strength R_m, the plasticity reserve coefficient, the ratio $(R_{p0,2})/(R_m)$ and the rupture stress R_B, as well as the elongation with the highest force A_g. FIG. 3 and TABLE 3 present the averaged values of the three static tensile tests for each of the examined orthodontic wires.

Among the tested orthodontic wires, the NiTi alloy one achieved the highest recorded elongation value at the highest force, $\overline{A_g}$ = 10.5% a few times higher result than the other examined wires. This alloy exhibited the lowest values of proof stress ($\overline{R_{p0,2}}$ = 346 MPa) and Young modulus ($\overline{E}$ = 37.6 GPa) (TABLE 3).

Already during the tensile tests, the NiTi wire underwent significant elongation and deformation (FIG. 3).

The alloy was probably reinforced already during the tests due to the plastic deformation and the formation of martensite, which strongly strengthened the alloy [31-33]. The plasticity reserve coefficient $\overline{R_{p0,2}}/\overline{R_m}$ equalled 0.29, the result two or three times higher than the other materials (the lower the value of this parameter, the higher the alloy's plasticity). The tensile strength ($\overline{R_m}$) of the NiTi wires was 1200 MPa.

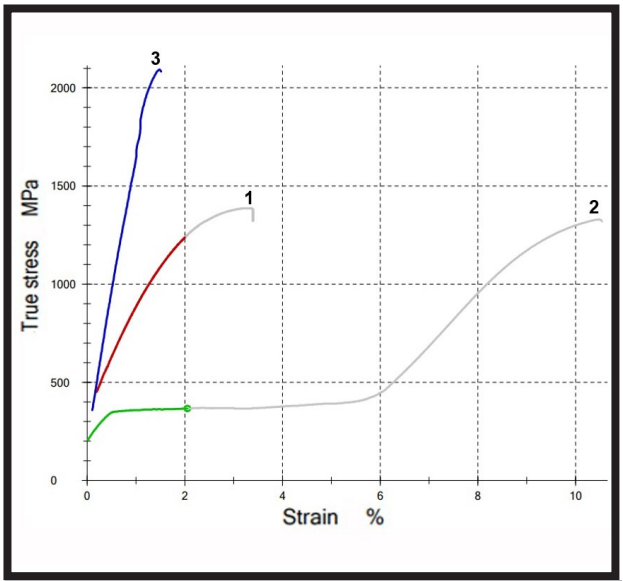

FIG. 3. Averaged waveforms of the static tensile test of the tested orthodontic wires. Curve 1 - Tiβ alloy wire, curve 2 - NiTi alloy, curve 3 - austenitic stainless steel of AISI 303 grade.

TABLE 3. Averaged values of the properties obtained from the tensile tests of the tested orthodontic wires.

Tested orthodontic wire	a_0, mm	b_0, mm	S_0, mm²	$\overline{E}$, GPa	$\overline{R_{p0,2}}$, MPa	$\overline{R_m}$, MPa	$\overline{R_{p0,2}}/R_m$	$\overline{R_B}$, MPa	$\overline{A_g}$, %
Tiβ (1)	0.40	0.55	0.22	62.8	965	1340	0.72	1270	3.2
NiTi (2)	0.50	0.50	0.25	36.7	346	1200	0.29	1190	10.5
Austenitic steel (3)	0.48	0.63	0.30	158.0	2020	2060	0.99	2050	1.5

The determined value $\overline{R_m}$ exceeded the upper limit of the values given by the producer (i.e. 800-1000 MPa) [25]. The NiTi rupture stress $\overline{R_B}$ was the lowest of all the tested materials and equalled ($\overline{R_B}$) = 1190 MPa (TABLE 3).

The highest tensile strength was exhibited by the rectangular wires made of austenitic steel grade AISI 303, whose value ($\overline{R_m}$) equalled 2060 MPa. This result is close to the lower limit guaranteed by the producer, i.e. 2190-2345 MPa [26]. For this material, the highest values of Young modulus were obtained ($\overline{E}$ = 158 GPa), significantly exceeding the values for the NiTi and Tiβ wires. The austenitic steel samples underwent the fastest rupture with the highest rupture stress ($\overline{R_B}$) = 2050 MPa and reached the lowest elongation of all the tested materials ($\overline{A_g}$ = 1.5%) (TABLE 3).

The Tiβ alloy, similarly to the austenitic steel, demonstrated a much lower elongation than of the nickel alloy with titanium $\overline{A_g}$ = 3.2%. For this alloy, the recorded tensile strength value was ($\overline{R_m}$) = 1340 MPa, which confirms the values declared by the producer, i.e. 1120-1320 MPa [25]. The significantly lower Young modulus values were also recorded ($\overline{E}$) = 62.8 GPa in comparison to austenitic steel which were still higher than those for NiTi. The mean value of the rupture stress for Tiβ equalled ($\overline{R_B}$) = 1270 MPa (TABLE 3).

The SEM observations of the orthodontic wire fractures were performed to evaluate the obtained surfaces and determine the morphology and topography of the analyzed materials in the area of their rupture. FIG. 4 shows SEM images of the fractography of the sample (wire) surfaces after the performed strength tests.

The fractography of the samples made of austenitic steel grade AISI 303 and Nitinol demonstrated a dimpled ductile fracture (FIG. 4a-d). Both the rectangular wire made of austenitic steel (FIG. 4a, b) and the NiTi one (FIG. 4c, d) formed necks which prove the material rupture (local reduction of the sample cross-section). The topography of the plastic fracture is characterized by a large set of dimples (craters) of different sizes and shapes.

The fractography of the Tiβ wire shows two kinds of fractures on the formed neck (FIG. 4e). A plastic fracture was formed on the external walls of the neck (FIG. 4f, g), while inside it, a brittle transcrystalline fracture was visible (FIG. 4f, h). The formed microcracks can propagate through the grains simultaneously in a few parallel and proximate planes of cleavage, followed by a formation of jogs (edges) visible on the fracture surface. Based on the observations, it can be concluded that the sample ruptured first on the internal side of the neck and next on the external sides.

In the further part of the study, electrochemical tests were performed with changing pH values. Three different corrosion environments were simulated. An artificial saliva solution was treated as an environment with the physiological 7.4 pH; the same solution with additions of HCl (for pH = 4.0, acid reaction), and of NaOH (for pH = 8.0, alkaline reaction) was used. For each of the tested orthodontic wires, the stationary potential was determined in the function of time (OCP) along with the polarization curves in the examined artificial saliva solution for three different solution pH values: 4.0, 7.4 and 8.0 (FIG. 5).

For the austenitic steel wire, the stationary potential was reached in each artificial saliva solution (FIG. 5a). The highest potential was recorded in the acidic environment (pH = 4.0), which means that in this solution austenitic steel has the highest corrosion resistance. A very similar potential value was reached by the sample in the environment with pH = 7.4. The lowest potential was reached by the steel sample in the environment with the highest alkaline pH (pH = 8.0).

For the NiTi arch, the change in the stationary potential in time is illustrated in FIG. 5b. The highest potential was reached in the artificial saliva solution with pH = 4.0 and it was maintained at this level (about 0.05 V vs Ag/AgCl) from the beginning of the measurement. In the case of pH = 7.4 and pH = 8.0, the stationary potential stabilized only after about 12 h. For pH = 7.4, the stationary potential values in the first 3 h were very unstable and varied in the scope of -0.15 to -0.5 V vs Ag/AgCl, after which the OCP values began to stabilize in the following hours. In the solution with pH = 8.0, the potential rapidly dropped after about 7 h from -0.5 V vs Ag/AgCl to -0.25 V vs Ag/AgCl, reaching a stable value of about -0.3 V vs Ag/AgCl after approx. 24 h.

The Tiβ wire (FIG. 5c) in each of the tested artificial saliva solutions was able to reach a stable stationary potential fast. The highest stationary potential was reached in the artificial saliva solution with pH = 7.4, which equalled about 0.01 V vs Ag/AgCl. The highest potential was assumed in pH = 4.0, it stabilized after about 4 h and equalled -0.35 V vs Ag/AgCl. FIG. 6a shows the polarization curve obtained for austenitic steel in the solution with free access to oxygen in the artificial saliva solution with three different pH values. One should note the curve obtained in the solution with pH = 4.0, in which both the cathodic and anodic current densities were higher as compared to the other solutions. There was also no distinguishable passivation area of the sample (FIG. 6a). This proved the lowest corrosion resistance of the austenitic steel wire in the solution with pH = 4.0. The largest passivation area from -0.15 to 0.7 V vs Ag/AgCl was exhibited by the steel sample in the artificial saliva solution with pH = 8.0. In turn, in the solution with pH = 7.4, a rapid current increase (a breakdown of the passive layer) took place with the potential 0.15 V vs Ag/AgCl (FIG. 6a).

In the case of alloy NiTi, the polarization curves (FIG. 6b) showed lower current values on the anodic side for each of the three artificial saliva solutions. The longest passivation area from about -0.3 V vs Ag/AgCl to 0.6 V vs Ag/AgCl was demonstrated in the artificial saliva solution with pH = 8.0. Nevertheless, there were no significant differences in the alloy corrosive behaviour depending on the solution pH, as was the case with austenitic steel. This was illustrated by the very similar curves in terms of shape.

The Tiβ alloy polarization curves (FIG. 6c), proved the highest corrosion resistance of all the examined materials.

The current densities on the anodic side were not much different from the cathodic side. Compared to the previous samples, the Tiβ alloy behaved similarly in each artificial saliva solution, regardless of its pH. The slightly lower current densities on the anodic side were obtained in the solution with pH = 4.0. The curves did not show a characteristic breakdown, a rupture of the corrosion resistance (rupture of the passive layer continuity). It was seen that the passivation area was large for titanium, i.e. from the value of 2.5 V vs Ag/AgCl, where only at about 1.75 V vs Ag/AgCl a characteristic increase in the anodic current density took place. This phenomenon occurred due to the titanium oxide TiO_2 transformation into Ti_2O_3 on the sample surface.

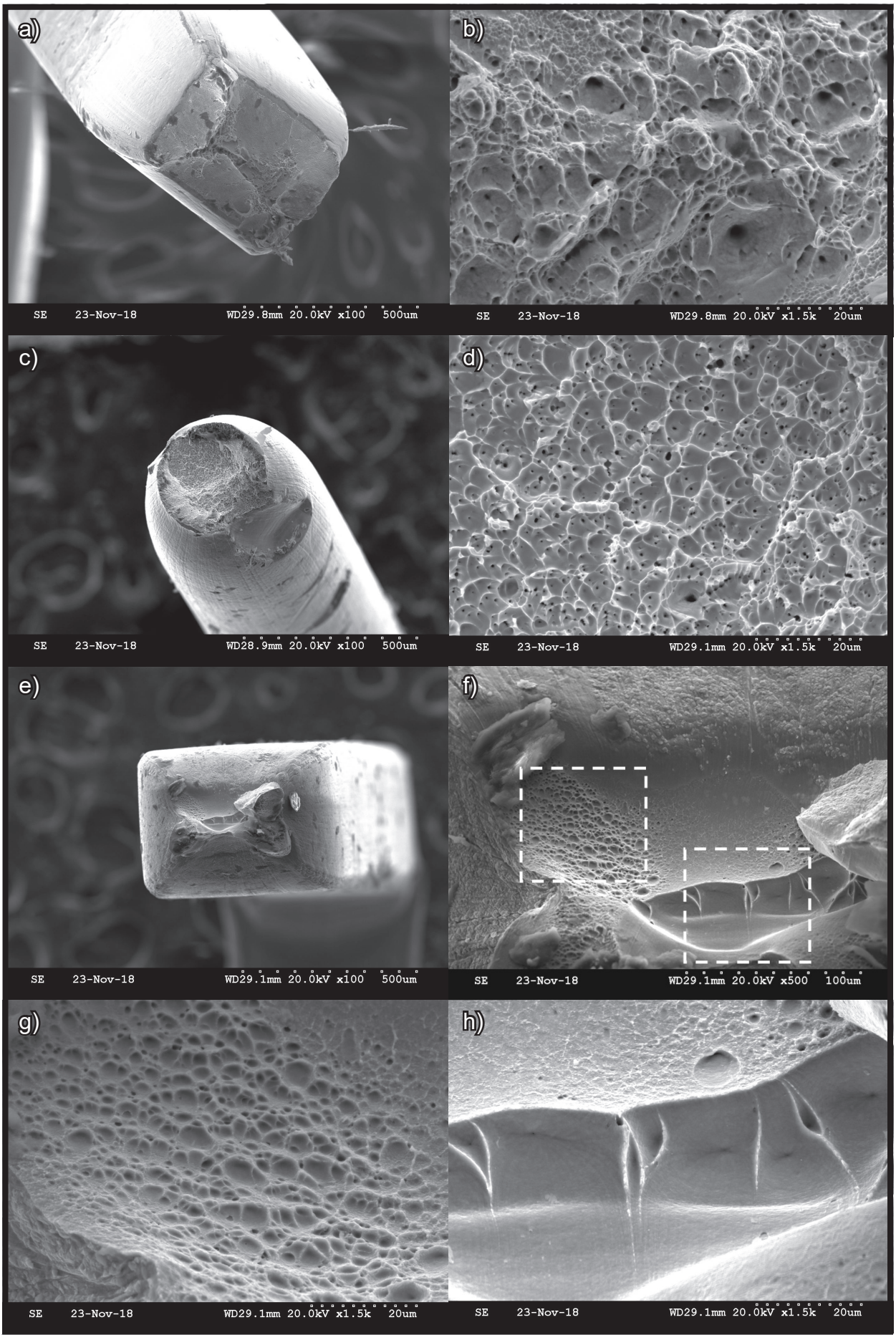

FIG. 4. SEM images of fractures of orthodontic wires: edge wire made of austenitic steel of AISI 303 grade (a and b), NiTi alloy (c and d), Tiβ alloy (e-h).

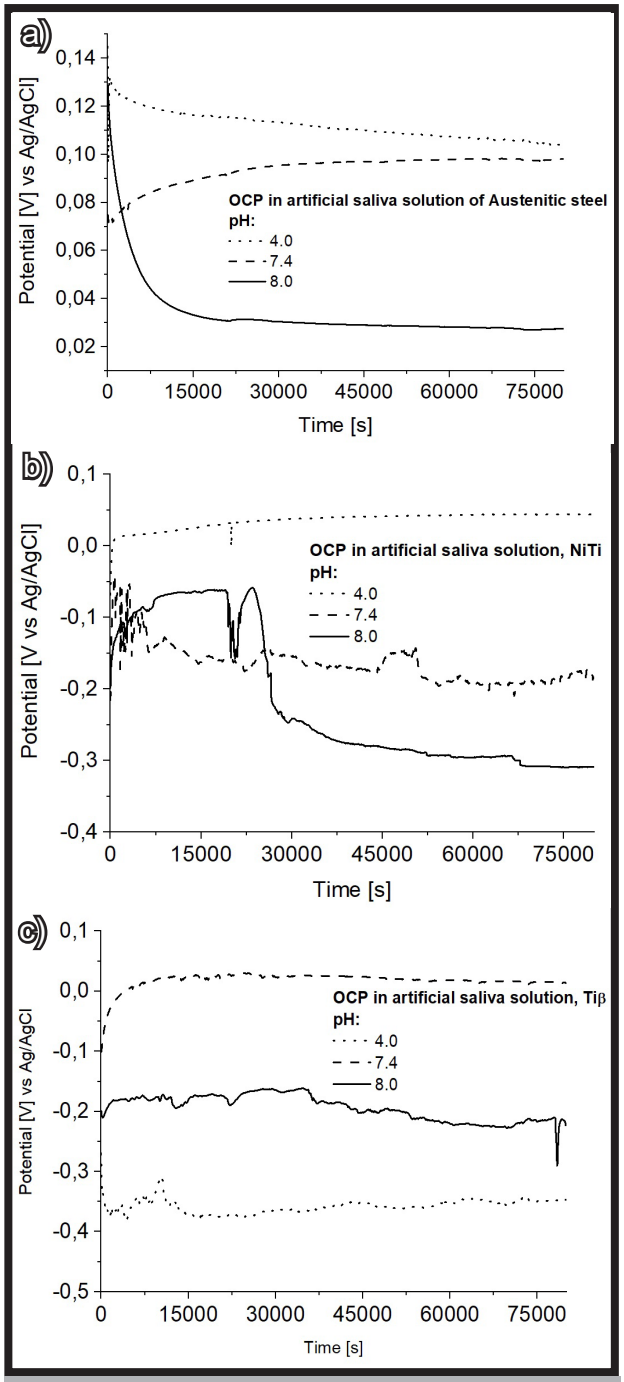

FIG. 5. Evolution of the corrosion potential vs. time determined for samples of austenitic steel of AISI 303 grade (a); Nitinol (b); Tiβ alloy, (c) in artificial saliva solution (different pH: 4.0, 7.4 and 8.0).

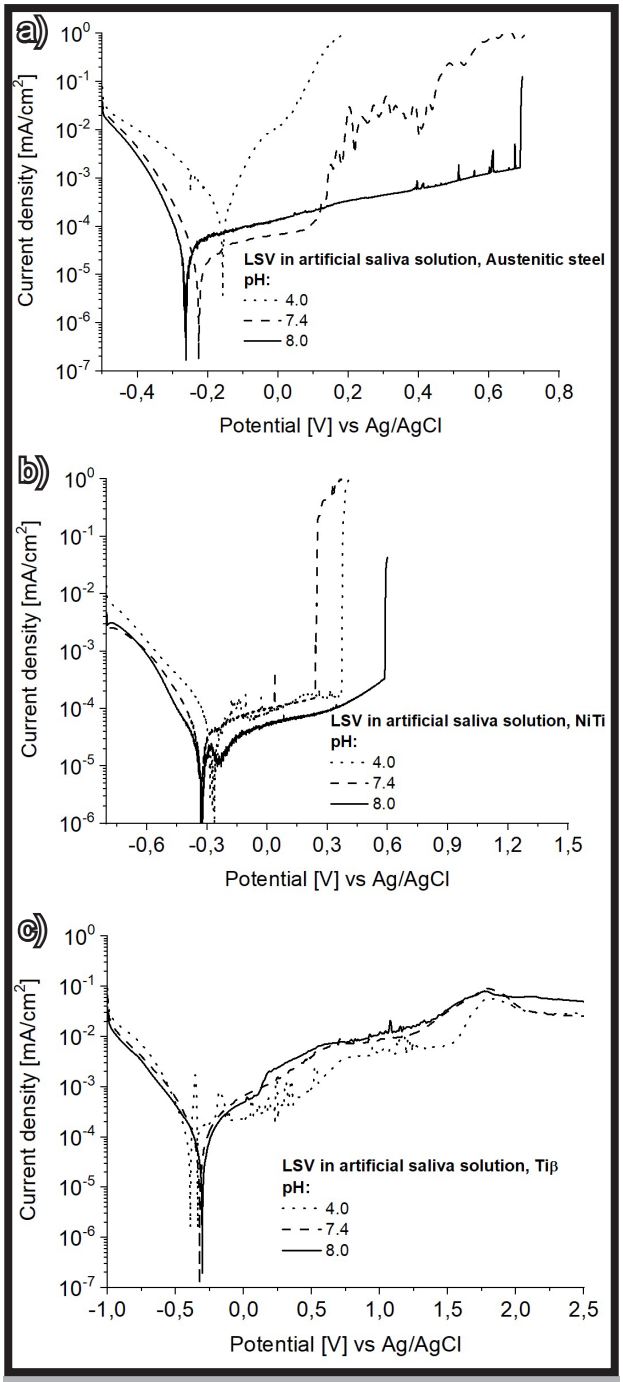

FIG. 6. Polarization curves obtained for samples of austenitic steel of AISI 303 grade (a), NiTi alloy (b) and Tiβ alloy, alloy (c) in artificial saliva solution (variable pH: 4.0, 7.4 and 8.0).

FIG. 7 compares the polarization curves for the three examined materials in the artificial saliva solution with pH = 7.4. We can see that Tiβ has a much broader scope of passivation potential than the other materials.

TABLE 4 shows a comparison of the tested materials in respect of the anodic current value with the potential 0 V vs Ag/AgCl and the width of the passivation potential scope. With the assumed potential, the highest resistance was exhibited by the austenitic steel grade AISI 303 wire (the lowest current density).

The obtained results were compared with other results described in the literature [34-36]. In [34], electrochemical tests showed that in the acidic environment (pH = 3.0) stainless steel wire had better corrosion resistance than nickel-titanium arc. In the present work, the austenitic steel and NiTi alloy wires reached a stable level of the stationary potential in the acidic environment (pH = 4.0), and for the Tiβ orthodontic wire, the highest stationary potential was observed for the alkaline environment (pH = 8.0). Future studies could concern microbiologically induced corrosion, similar to the one presented in [35,36].

TABLE 4. Anodic current density for the tested orthodontic wires at the potential of 0 V vs Ag/AgCl in artificial saliva solution at pH = 7.4.

Orthodontic wires	Current density·10^{-5} [mA/cm^2]	The area passivation [V] vs Ag/AgCl
Austenitic steel	6.2	-0.15 - 0.07
NiTi	9.9	-0.24 - 0.23
Tiβ alloy	61.9	-0.06 - 2.5 (in the range tested)

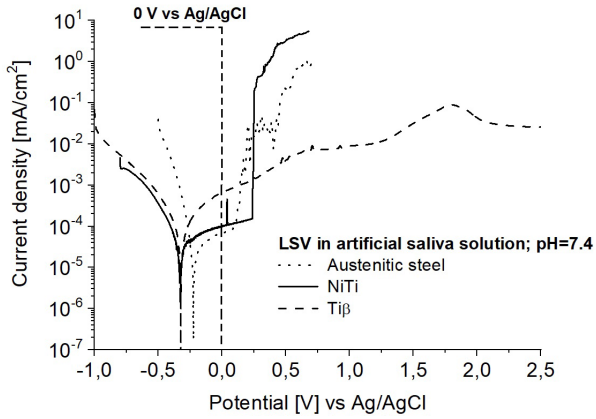

FIG. 7. Comparison of LSV of austenitic steel of AISI 303 grade, NiTi and titanium alloy β in artificial saliva solution with pH = 7.4.

Conclusions

The performed static tensile tests, observations of the fractures and electrochemical examinations of three different wires used in the orthodontic treatment made it possible to draw the following conclusions:

The performed strength tests showed that the highest tensile strength ($\overline{R}_m$ = 2060 MPa) and Young modulus ($\overline{E}$ = 158 GPa) was exhibited by the rectangular orthodontic wire made of austenitic steel grade AISI 303. The best plastic properties were demonstrated by the NiTi alloy wire ($\overline{A}_g$ = 10.2 %).

After a rupture, the SEM examinations of the sample fractures revealed a dimpled ductile fracture both for the austenitic steel wire and the NiTi wire. In the case of alloy Tiβ, a mixed fracture was revealed (ductile, formed on the external sides of the neck, and brittle transcrystalline, formed inside).

The electrochemical tests of the corrosion stationary potential change in time revealed the austenitic steel and NiTi wires stable stationary potential in the acidic environment. The Tiβ samples exhibited the highest stationary potential in the alkaline environment.

The performed electrochemical tests of the stationary potential and the polarization curves confirmed that all the materials in the examined artificial saliva solution were passivated in the scope of the potential they operated in freely when submerged in the solution.

The highest current density was observed for the Tiβ wire. Nevertheless, of the three examined biomedical materials it was also the Tiβ wire, which demonstrated the highest corrosion resistance, due to the widest passivation scope.

The corrosion polarization investigations helped determine the corrosion rate. For austenitic steel and NiTi, the broadest passivation area occurred in the solution with pH = 8.0.

The comparison of the polarization curves of the examined samples obtained during the tests in the artificial saliva solution with pH = 7.4 showed that the Tiβ wire had the broadest passivation area in the specified potential scope.

Acknowledgements

The authors would like to thank Joanna Loch-Zawrotniak for her help with laboratory preparation.

The work has been implemented within the framework of statutory research of the AGH University of Science and Technology, contract No 16.16.110.663.

ORCID iDs

J. Augustyn-Nadzieja: https://orcid.org/0000-0002-3614-0609
A. Szczotok: https://orcid.org/0000-0003-0680-0837

References

[1] Shaw W.C., Richmond S., O'Brien K. D., et al.: Quality control in orthodontics: indices of treatment need and treatment standards. British Dental Journal 170 (1991) 107-112.
[2] Liu Z., McGrath C., Hägg U.: The impact of malocclusion/orthodontic treatment need on the quality of life: a systematic review. Angle Orthodontist 79 (3) (2009) 585-591.
[3] Fischer T.J.: Orthodontic treatment acceleration with corticotomy--assisted exposure of palatally impacted canines: a preliminary study. Angle Orthodontist 77 (3) (2007) 417-420.
[4] Porównanie metod stosowanych w ortodoncji. Kliniki.pl (29th November, 2020)
[5] 60 procent osób w Polsce ma wady zgryzu. prawo.pl (29th November, 2020)
[6] Allen K.R.: Methods of testing the mechanical properties of orthodontic wires. A report submitted in partial fulfilment of the requirements for the degree of Master of Dental Surgery, Department of Dentistry Faculty of Dentistry, The University of Adelaide South Australia, 1994.
[7] Khamatkar A.: Ideal Properties of Orthodontic Wires and Their Clinical Implications - A Review. Journal of Dental and Medical Sciences 14 (1) (2015) 47-50.
[8] Petrini L., Migliavacca F.: Biomedical applications of shape memory alloys. Journal of Metallurgy 2011 (2011) 1-15.
[9] Petrini L., Migliavacca F., Massarotti P., Schievano S., Dubini G., Auricchio F.: Computational studies of shape memory alloy behavior in biomedical applications. Journal of Biomechanical Engineering 125 (4) (2005) 716-725.
[10] Kotha R.S., Alla R.K., Shammas M., Ravi R.K.: An Overview of Orthodontic Wires. Trends in Biomaterials and Artificial Organs 28 (1) (2014) 32-36.
[11] Pelsue B.M., Zinelis S., Bradley T.G., Berzins D.W., Eliades T., Eliades G.: Structure, composition, and mechanical properties of australian orthodontic wires, Angle Orthodontist 79 (1) (2009) 97-101.
[12] Andriekute A., Vasiliauskas A., Sidlauskas A.: A survey of protocols and trends in orthodontic retention. Progress in Orthodontics 18 (31) (2017) 1-8.
[13] Wang Y., Liu C., Jian F., McIntyre G.T., Millett D.T., Hickman J., Lai W.: Initial arch wires used in orthodontic treatment with fixed appliances (Review). The Cochrane Collaboration. Published by John Wiley & Sons, Ltd., 2018
[14] Pataijindachote J., Juntavee N., Viwattanatipa N.: Corrosion analysis of orthodontic wires: an interaction study of wire type, pH and immersion time. Advances in Dentistry & Oral Health 10 (1) (2018) 1-7.
[15] Verstryngea A., Humbeeckb J. V., Willemsc G.: In-vitro evaluation of the material characteristics of stainless steel and beta--titanium orthodontic wires. American Journal of Orthodontics and Dentofacial Orthopedics 130 (4) (2006) 460-470.
[16] Castro S.M., Ponces M.J., Lopes J.D., Vasconcelos M., Pollmann M.C.F.: Orthodontic wires and its corrosion - The specific case of stainless steel and beta-titanium. Journal of Dental Sciences 10 (1) (2015) 1-7.
[17] Cempel M., Nikel G.: Nickel: A review of its sources and environmental toxicology. Polish Journal of Environmental Studies 15 (3) (2006) 375-382.
[18] Rahilly G., Price N.: Nickel allergy and orthodontics. Journal of Orthodontics 30(2) (2003) 171-174.
[19] Fadlallah S.A., El-Bagoury N., Gad El-Rab S.M.F., Ahmed R.A., El-Ousamii G.: An overview of NiTi shape memory alloy: Corrosion resistance and antibacterial inhibition for dental application. Journal of Alloys and Compounds 583 (2014) 455-464.
[20] Barcelos A.M., Luna A.S., Ferreira N., Castro Braga A.V., Baptista do Lago D.C; Ferreira de Senna L.: Corrosion evaluation of orthodontic wires in artificial saliva solutions by using response surface methodology. Materials Research 16 (1) (2013) 50-64.
[21] Surowska B., Weroński A.: Struktura i własności biomateriałów. (In Polish) Prace Naukowe Politechniki Lubelskiej 219 (1995) Mechanika 50.
[22] Eliaz N.: Corrosion of metallic biomaterials: A review. Materials 12 (3) (2019) 1-91.
[23] Świeczo-Żurek B.: Biomaterials. (in Polish) Wydawnictwo Politechniki Gdańskiej (2009).
[24] Loch J.: Corrosive behavior of biomedical titanium alloys in simulated physiological solutions. Doctoral dissertation, Kraków, 2017 (in Polish).
[25] https://www.ortodonta.info/
[26] https://www.falconpolska.com
[27] PN-EN 10002-1: Metals - Tensile test - Test method at ambient temperature, 2002 (in Polish).
[28] Małkiewicz K., Boryczko W., Sztogryn M., Kamiński J., Wierzchoń T.: Assessment of corrosion processes in steel orthodontic archwires – in vitro studies. Ortodontic Forum 15 (2019) 95-103.
[29] ISO 10271:2001 Dental metallic materials - Corrosion test methods (2001).
[30] Bolla V.L., Munnangi S.R., Kumar M.M.G, Chowdary U.K., Koppulu P., Swapna L.A.: Correlation between the pH of saliva, plaque and buffering capacity of saliva. International Journal of Applied Dental Sciences 3(4) (2017) 48-50.
[31] Choi W.S., Pang E.L., Ko W-S., Jun H., Bong H.J., Kirchlechner Ch., Raabe D., Choi P-P.: Orientation-dependent plastic deformation mechanisms and competition with stress-induced phase transformation in microscale NiTi. Acta Materialia 208 (2021) 1-11.
[32] Chen Y., Tyc O., Molnárová O., Heller L., Šitter P.: Tensile deformation of superelastic NiTi Wires in wide temperature and microstructure ranges. Shape Memory and Superelasticity 5 (2019) 42-62.
[33] Song D., Kang G., Kan Q., Yu Ch., Zhang Ch.: The effect of martensite plasticity on the cyclic deformation of super-elastic NiTi shape memory alloy. Smart Materials and Structures 23 (1) (2014) 1-7.
[34] El Kouifat M.K., Ouaki B., El Hajjaji S., El Hamdouni Y.: Corrosion of Orthodontic Arch-Wires in Artificial Saliva Environment. Journal of International Dental and Medical Research 11 (3) (2018) 786-790.
[35] Trolić I.M., Turco G., Contardo L., Serdarević N.L., Otmačić Ćurković H., Špalj S.: Corrosion of Nickel-Titanium Orthodontic Archwires in Saliva and Oral Probiotic Supplements. Acta Stomatologica Croatica 51(4) (2017) 316-325.
[36] Trolić I.M., Serdarević N.L., Todoric Z., Budimir A., Spalj S., Otmačić Ćurković H.: Corrosion of orthodontic archwires in artificial saliva in the presence of Lactobacillus reuteri. Surface & Coatings Technology 370 (2019) 44-52.

MONITORING VITAL FUNCTIONS OF A-375 MELANOMA CELL CULTURES VIA THIN-FILM NICKEL CAPACITORS

Aleksandra Wilczyńska[1], Andrzej Kociubiński[1*], Dawid Zarzeczny[1], Maciej Szypulski[1], Dominika Pigoń[2], Teresa Małecka-Massalska[2], Monika Prendecka-Wróbel[2]

[1] Lublin University of Technology, Nadbystrzycka 38A, 20-618 Lublin, Poland
[2] Medical University in Lublin, Radziwiłłowska 11, 20-080 Lublin, Poland
*e-mail: akociub@semiconductor.pl

Abstract

This article deals in the constantly developing branch of microelectronic devices used in various fields of medicine, i.e. diagnostics and treatment of previously incurable human diseases. A method for assessing and monitoring the vital functions of living cells by measuring cellular impedance in real-time using the ECIS® system and a commercial culture substrate is presented. The goal was to develop a substrate significantly less expensive than a commercial substrate that would be suitable for multiple uses and compatible with the ECIS® measurement station. Moreover, thanks to the use of a material with electrochemical properties other than the biocompatible material (gold or platinum) it is possible to observe the cells behavior with regard to the toxic agent. For this purpose, a culture substrate with nickel comb capacitors was used. To make the electrodes, a thin metal layer was sputtered on polycarbonate plates in the magnetron sputtering process. Prior to the next stages, technological masks were designed so as to fit in the ECIS® measuring station. Subsequently, the microelectronic processes of photolithography and etching the metal layer were performed. Finally, the wells were glued onto the culture medium with a biocompatible adhesive. The completed substrates were transferred to the Department of Human Physiology, Medical University of Lublin, for the culture test on A-375 human melanoma cells. The results of the experiment determined the usefulness of the device for monitoring cell culture vital functions by means of impedance measurement.

Keywords: *ECIS, nickel, thin layers, melanoma, magnetron sputtering*

[Engineering of Biomaterials 157 (2020) 10-14]

doi:10.34821/eng.biomat.157.2020.10-14

Introduction

Over the last few years, there has been much progress in the development of medical measuring devices due to the increasing number of incurable diseases in the modern world. The novel microelectronic technologies and strategies are to limit animal testing and yet allow monitoring cellular changes at the molecular level resulting from external stimuli or administered pharmacological agents [1-3].

One of the methods to assess the condition of cell culture is to measure its electrical parameters. This is a completely non-invasive technique, performed *in vitro*, which enables the relative determination of the number of cells in all the tested samples. Therefore, the obtained test results are accurate and quantitative [4].

The ECIS® impedance detection between the cell and the electrical substrate is a popular technique based on measuring the ratio of voltage and current in AC circuits using a sinusoidal signal [5-6].

This paper presents the results of a study conducted on a nickel electrical circuit with a suspension of A-375 melanoma cells deposited on its surface. The ECIS® technique consists in measuring the amount of the current flowing and the amount blocked by the culture cell membranes adjacent to the electrode surface. Due to the life cycles of cells and their ability to migrate, the experiments results changed proportionally to the impedance changes. Due to the possible long-term monitoring of the vital cells functions, the ECIS® method is gaining popularity among biological and chemical laboratory tests [7].

Materials and Methods

ECIS® apparatus in the study of cells vital functions

The ECIS® cell impedance measurement consists in using a biocompatible substrate on the surface of which there are 8 wells with thin-film comb capacitors. This technique has been widely used in *in vitro* studies to perform the cells behavior qualitative assessment. Microorganisms are tested in terms of multiplication, migration, barrier functions, transduction effects, cell invasiveness, cell response to toxins, electroporation effect, and many others [1]. The capacitors and cells can be converted to an equivalent electrical circuit containing a resistor and a capacitor. The capacitance of the capacitor surface can be treated as the capacitance of the well containing the cell culture medium. The electrode resistance prevails over the well resistance, whose value is oppositely proportional to the capacitor surface area. A simplified mathematical model of the ECIS® system is further discussed in the publication [8].

Tests performed on the ECIS® system begin with applying a culture medium onto the electrode surface. Then the cell culture is introduced and it enters phase 1 of its life cycle. In this phase, cells stick to the bottom of the well and begin to grow and multiply, thanks to a properly selected medium. The impedance increase depends on the decreasing free space on the capacitors surface occupied by non-conductive cell membranes [6]. In phase 2, the cells stabilize, which results in a virtually unchanging impedance value. The minimal increase or decrease in the value comes from the culture movement and the cells finding free spaces on the electrode surface. In phase 3, there is a decrease in resistance and, similarly, an increase in capacity due to cell death and the loss of their adhesive properties with the substrate [7]. The three phases of the cell life cycle are shown in FIG. 1 by the measured values of resistance and capacity during 35 h of the culture.

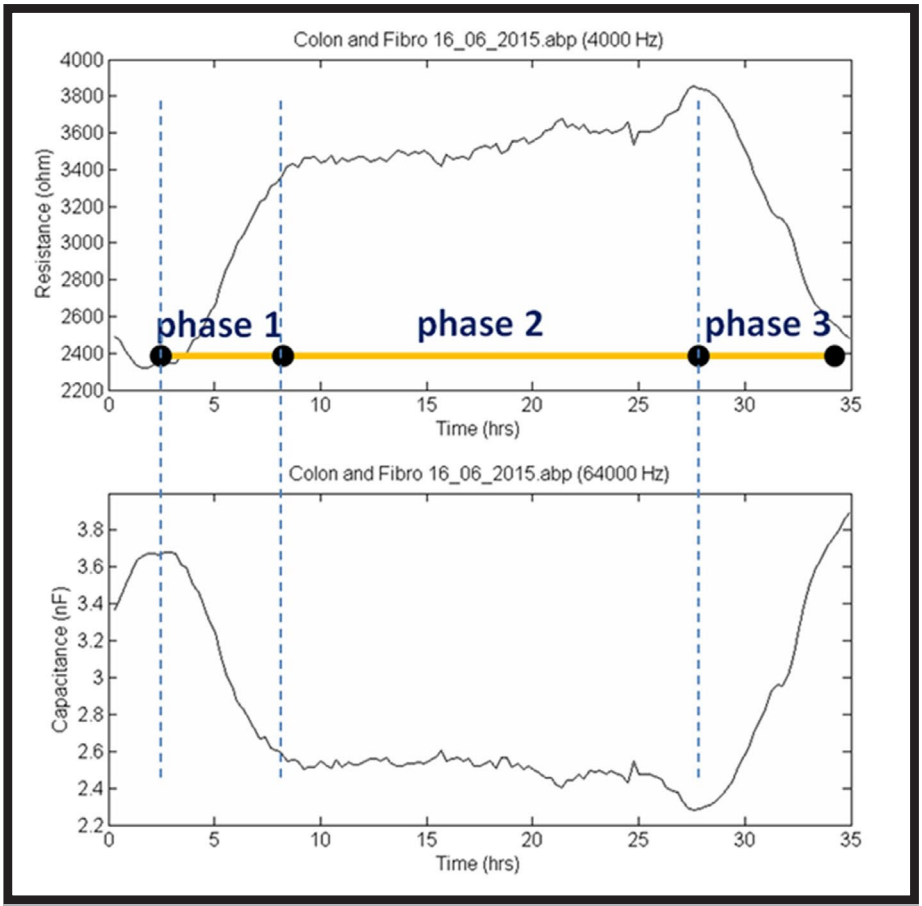

FIG. 1. Results of measurements of resistance (f = 4 kHz) and capacitance (f = 64 kHz) measured using a commercial ECIS® substrate [7].

Nickel

In order to obtain the test substrate, it was necessary to match the electrode size of the comb capacitor to the cells size. Commercial ECIS® plaques only use polyethylene terephthalate (PET) or polycarbonate (PC) substrates with gold or platinum measuring electrodes. The ECIS® apparatus also makes it possible to study the effects of heavy metals, as their properties are different from those of biocompatible metals measured on living cells. However, in order to carry out such tests, it was necessary to create dedicated measurement structures from other metals [9-11].

Biocompatibility is crucial in the case of prolonged contact with metal, e.g. implants. However, in many applications (e.g. qualification tests) the material has a short-term direct contact with the patient or organic material. In this paper, the aim is to create test substrates with nickel electrodes used to monitor the vital cells functions using the ECIS® measuring station and thus replace much more expensive commercial substrates.

Nickel and its alloys, due to their electrical properties, have been widely used in electronic microcircuits. Due to its high resistance to elevated temperatures, nickel is readily used in electroplating processes [12]. Advances in technology have led to the development of metal neural probes. One of such probes consists of a nickel shaft made via the electroplating process [11]. Additionally, diagnostic purposes often require elevated temperatures. In order to meet these requirements, a nickel micro-heater has been developed, which can maintain the operating temperature of 250°C throughout the duration of the experiment [13]. Nickel is also used in the CellTracks cell analysis system [14].

Metallization

In order to deposit a thin layer of metal, the magnetron sputter deposition of nickel was carried out on a 2 mm thick rectangular polycarbonate plate. This technique is based on the evaporation of material particles coming from the source (target) under the influence of ionized electromagnetic field energy of inert gases (in this case argon). The process temperature did not exceed 70°C so as not to damage the substrate material. Before initiating the atomization process, it was necessary to obtain a sufficiently high vacuum of 10^{-7} Torr. As a result, a nickel layer with a thickness of ~100 nm was obtained.

Design of technological masks and the etching process of photosensitive emulsions and metal

As part of the experiment, the test substrates with nickel electrodes were made. The first step was to design technological masks that were modeled on a commercial electrode system with eight wells. Each pair of electrodes was made as a 6-finger comb capacitor, the width of a single finger and the distance between them measured 200 µm. The second step was to apply a photosensitive emulsion to the sputtered nickel layer. In the photolithography process, the photosensitive emulsion was exposed to UV radiation through the mask. Then, the etching of the emulsion and metal layers was performed with chemical reagents. The final step was to clean the substrate in an ultrasonic washer, fix the wells to the culture media with biocompatible silicone, and sterilize them with ultraviolet radiation. FIG. 2 shows the electrode array with 8 wells.

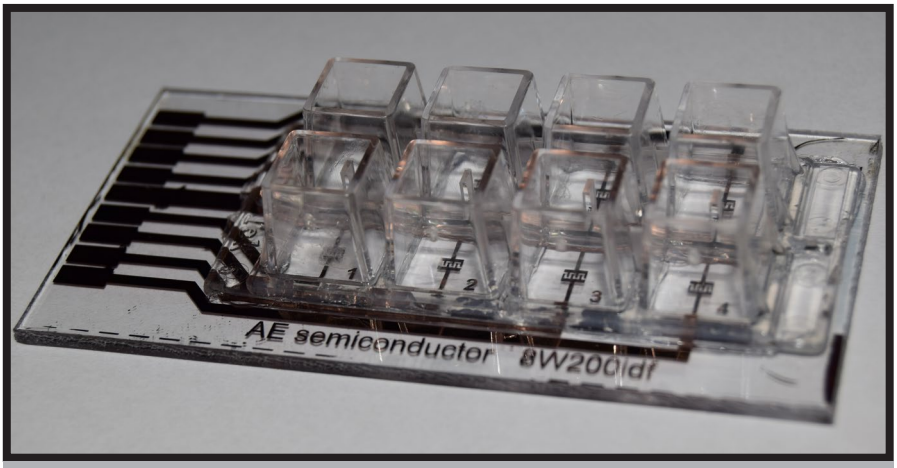

FIG. 2. Ready-made nickel cell culture medium.

The course of the experiment on cell culture of A-375 melanoma

The substrates were used for the experimental cell culture at the Department of Human Physiology of the Medical University of Lublin, using melanoma tumor cells derived from human skin tissue. The culture came from the American Type Culture Collection (ATCC) organization and the medium was Dulbecco's Modification of Eagle's Medium (DMEM) [15]. The cells were grown under controlled growth conditions with constant humidity and 5% CO_2 air saturation.

600 µl of the DMEM culture medium was applied to every well to check their good leakage. Then the matrices were fixed in the measuring station and placed in an incubator under appropriate conditions. The electrical parameters calibration was performed at 4 kHz. After 24 h, the culture medium was removed from the wells and replaced with 540 µl of the fresh medium along with bovine serum and 60 µl of the cell suspension in six wells. The pure reference medium was introduced in the remaining two wells. The cell culture matrices were placed in the ECIS® measuring station for over 160 h (FIG. 3).

FIG. 3. Nickel matrices with A-375 melanoma cell culture (left) in the ECIS® measuring station.

Results and Discussions

In our work, we determined the possibility of using innovative nickel electrodes to measure changes in electrical parameters in the culture of A-375 human melanoma cells. Using the ECIS® system we recorded important changes in resistance, impedance, and capacitance in the A-375 cell culture.

Monitoring the impedance changes in cell cultures is of great importance in biological sciences, medicine but also in technical fields, regarding the biomaterials development and modification for implants [16] or cell–semiconductor interfaces [17] where the cell attachment is an important parameter. Accordingly, the experimental means to monitor the attachment and spreading of animal cells to artificial surfaces are most valuable [18].

There are two electrodes in the ECIS® device: a large common reference electrode and a small working electrode. In our experiment, the A-375 line cells were cultured in a holder and measured using nickel electrodes. During the culture, the cells attachment and spread on the electrode surface change the impedance value in such a way that morphological information of the attached cells can be inferred. That is why the cells behavior is an important factor for this type of biosensor [18]. Adherent cells, e.g. melanoma, attach to a surface before they grow and proliferate. Having attached, the cells are no longer spherical, they become flat [19], which affects the impedance.

The obtained results prove that melanoma cells effectively grow on the electrodes used in the study (FIGs. 4-7). Depending on the cells type (a cancer cell or a normal cell), their growth, proliferation and then death are reflected in the changes in impedance and capacitance over time. One of the major difficulties to study those processes is to differentiate between adhesion, spreading, and proliferation. Wegener et al. [18] described in detail the use of a combination of resistance and capacitance to distinguish between those parameters. Our results coincide with Wegener's observations and complement each other. The obtained impedance values (FIG. 5) show an upward trend throughout the almost entire experiment duration (nearly 160 hours). The hours 10-90 reflect the proliferation and migration of cells on the electrode surfaces. The resulting impedance values increase from about 7010 Ω to 7090 Ω during this period. As it can be noted in FIG. 4 there are clear impedance fluctuations expressed in small peaks, which reflects the cells movement. This strongly corresponds to the previous observations presented in FIG. 1 representing fibroblasts movement and growth on gold electrodes in the ECIS® device. Alternations in the cell behavior after attachment (spreading, proliferation, micromotions) result in impedance changes [20]. Electrical impedance is defined as the opposition to an electrical current within a circuit. In direct current systems, the impedance is simply the resistance. In alternating current systems, the changing electric and magnetic fields create additional and varying opposition to the applied current [21]. This is consistent with the resistance measurement results (FIG. 5) obtained during our experiment.

The decrease in capacitance (FIG. 6) and the resistance increase correspond to the cell proliferation, the recorded values complement each other. The measured capacitance at 64 kHz decreases with the increasing surface coverage, which is useful for assessing the cells spread on the electrode surface. These results are consistent with the results of Wegener's [18] studies on MDCK cells (epithelial cell line derived from the canine kidney) on gold electrodes.

The obtained results of electrical parameters are reflected in the microscopic image presented in FIG. 7 with an almost confluent layer of cells on the electrodes surface. However, it should be noted that the experiment was conducted on melanoma cells that have high metastatic potential. The reason for using this type of cells was their high viability *in vitro*. Having improved the technology of non-gold electrodes production, the more demanding cells characterized by the less stable growth may be used for future tests.

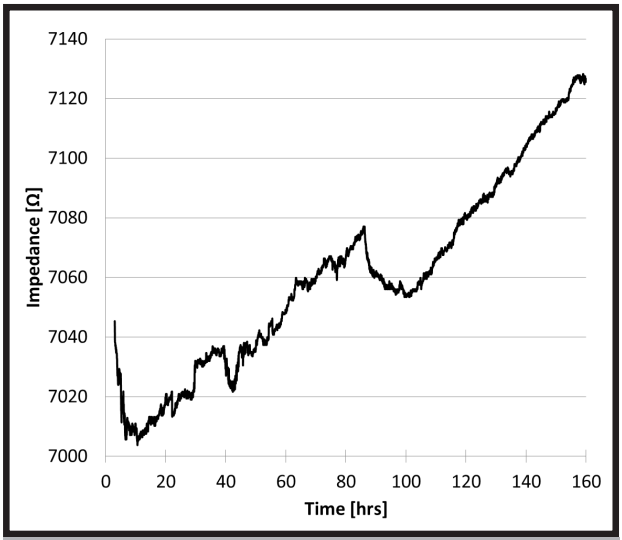

FIG. 4. Impedance measured with a nickel matrix at 16 kHz for over 160 h.

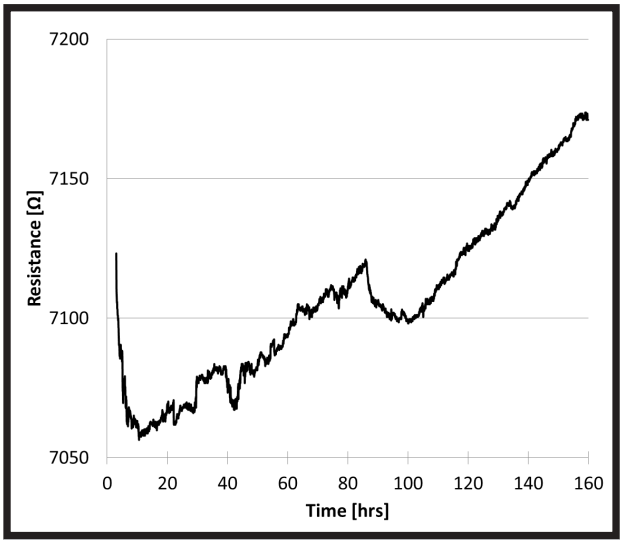

FIG. 5. Resistance measured with a nickel matrix at 4 kHz for over 160 h.

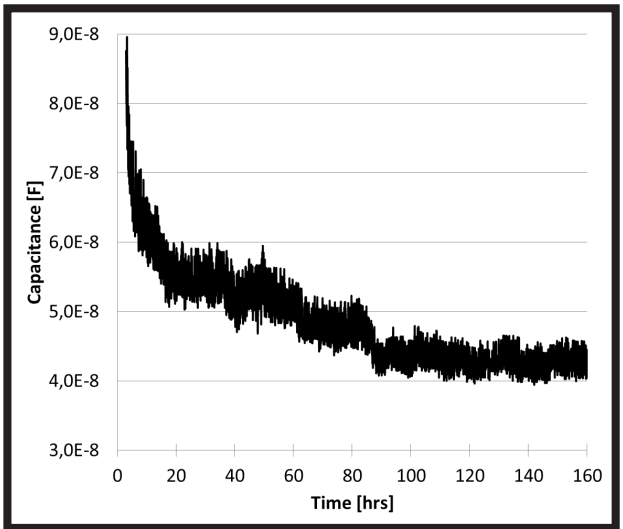

FIG. 6. Capacitance measured with a nickel matrix at 64 kHz for over 160 h.

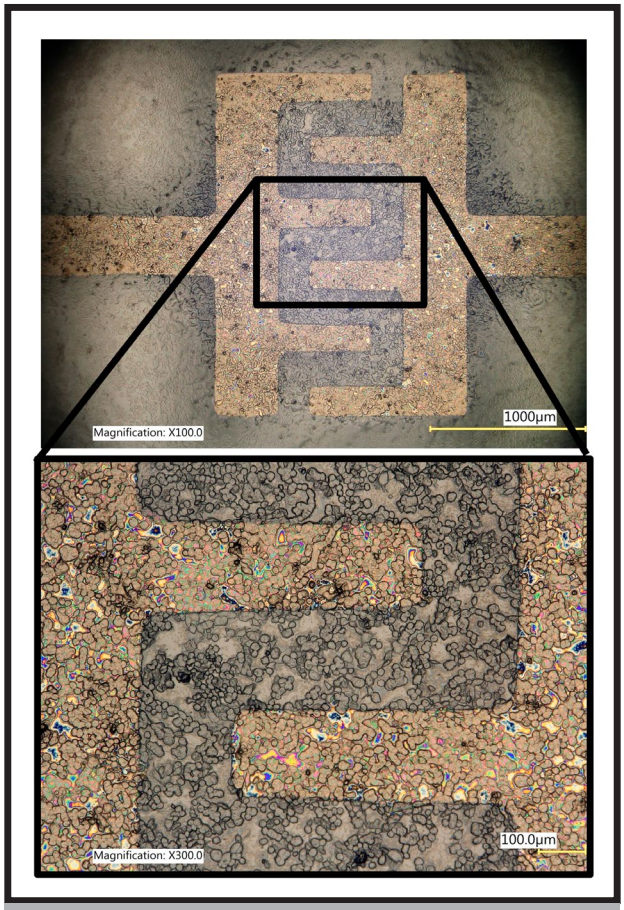

FIG. 7. Nickel capacitor electrode with cell culture after more than 160 h of the experiment.

Conclusions

The above article presents a non-standard technology to obtain the measuring medium with thin-film nickel comb capacitors applicable in the ECIS® apparatus. Prior to performing the test cultures, the substrates were checked for compatibility with the measurement station. Due to its high *in vitro* viability, the A-375 melanoma cell culture was used for the experiment. Thanks to this, it was possible to check whether the toxic nature of nickel would allow monitoring the vital functions of cells. In this experiment, we found that nickel electrodes can be used to study cells. Nickel electrodes in the ECIS® system do not inhibit proliferation and are not cytotoxic to A-375 cells. The correct course of the cell cycle indicates that nickel electrodes may be used to study the material's influence on living cells. In addition, our results prove that nickel can be used as a cheaper material for many applications that have direct contact with the living organism.

Acknowledgments

This work was financed from the statutory funds of the Department of Electronics and Information Technology of Lublin University of Technology.

ORCID iDs
A. Wilczyńska: https://orcid.org/0000-0002-5630-1078
A. Kociubiński: https://orcid.org/0000-0002-0377-8243
D. Zarzeczny: https://orcid.org/0000-0003-2029-9962
M. Szypulski: https://orcid.org/0000-0002-6227-3624
D. Pigoń: https://orcid.org/0000-0002-7545-3237
T. Małecka-Massalska: https://orcid.org/0000-0003-3384-0324
M. Prendecka-Wróbel: https://orcid.org/0000-0001-9414-4344

References

[1] https://biophysic.com [access: 12.12.2020]
[2] Rack H.J., Qazi J.I.: Titanium alloys for biomedical applications. Materials Science and Engineering C 26 (2006) 1269–1277.
[3] Chalklen T., Wuinhshen J., et al.: Biosensors Based on Mechanical and Electrical Detection Techniques. Sensors 20 (2020) 5606.
[4] Xu Y., Xie X., Duan Y., Wang L., Cheng Z., Cheng J.: A Review of Impedance Measurements of Whole Cells. Biosensors and Bioelectronics 77 (2016) 824–836.
[5] Giaever I., Keese C.R.: A Morphological Biosensor for Mammalian Cells. Nature 366/6455 (1993) 591–592.
[6] Voiculescu I., Toda M., Inomata N., Ono T. Li F., Nano and Microsensors for Mammalian Cell Studies. Micromachines 9 (2018) 439.
[7] Kociubiński A. et al.: Real-time Monitoring of Cell Cultures with Nickel Comb Capacitors. Informatics, Control, Measurement in Economy and Environmental Protection 2 (2020) 32–35.
[8] Caide Xiao, John H.T. Luong: A simple mathematical model for electric cell-substrate impedance sensing with extended applications. Biosensors and Bioelectronics 25 (2010) 1774-1780.
[9] Crowell L., Yakisich J., et al.: Electrical Impedance Spectroscopy for Monitoring Chemoresistance of Cancer Cells. Micromachines 11 (2020) 832.
[10] Arias L.R., Carla A.P., Yang L.: Real-Time Electrical Impedance Detection of Cellular Activities of Oral Cancer Cells. Biosensors and Bioelectronics 25(10) (2010) 2225–2231.
[11] Scholten K., Meng E.: Materials for Microfabricated Implantable Devices: A Review. Lab on a Chip 15(22) (2015) 4256–4272.
[12] Serek A., Budniok A.: Otrzymywanie i własności elektrolitycznych warstw kompozytowych na osnowie niklu zawierających tytan. Wyd. Uniwersytetu Śląskiego, Instytut Fizyki i Chemii Metali 3 (2002) 63–67.
[13] Bhattacharyya P., Basu P.K., Mondal B., Saha H.: A low power MEMS gas sensor based on nanocrystalline ZnO thin films for sensing methane. Microelectronics Reliability 48 (2008) 1772–1779.
[14] Kagan M. et al.: CellTracks: Cell Analysis System for Rare Cell Detection. Proceedings SPIE, Clinical Diagnostic Systems: Technologies and Instrumentation 4625 (2002) 20–28.
[15] https://www.lgcstandards-atcc.org/products/all/CCL1.aspx#culturemethod [access: 13.12.2020]
[16] Vogler E.A.: Thermodynamics of short-term cell adhesion in vitro. Biophysical Journal 53 (1988) 759–769.
[17] Parak W.J. et al.: Electrically excitable normal rat kidney fibroblasts: A new model for cell–semiconductor hybrids. Biophysical Journal 76 (1999) 1659–1667.
[18] Wegener J., Keese C.R., Giaever I.: Electric cell–substrate impedance sensing (ECIS) as a noninvasive means to monitor the kinetics of cell spreading to artificial surfaces. Experimental Cell Research 259 (2000) 158–166.
[19] Mohanty S.P.: Biosensors: A Survey Report. Citeseer (2001) 1–15.
[20] Xiaoqiu H., Nguyen D., Greve D.W., Domach M.M.: Simulation of microelectrode impedance changes due to cell growth. IEEE Sensors Journal 4/5 (2004) 576–583.
[21] Coffman F.D., Cohen S.: Impedance measurements in the biomedical Sciences. Analytical Cellular Pathology 35 (2012) 363–374.

MAY METALLIC BIOMATERIALS USED FOR ORTHOPAEDIC IMPLANTS PROMOTE CARCINOGENESIS? PRELIMINARY TRANSCRIPTOMIC RESEARCH ON HUMAN CHONDROCYTES

Magdalena Walkowiak-Przybyło*

Institute of Materials Science and Engineering,
Lodz University of Technology,
Stefanowskiego 1/15, 90-924 Łódź, Poland
*e-mail: magdalena.walkowiak-przybylo@p.lodz.pl

Abstract

The aim of this research was to assess the risk of carcinogenesis induced by the metallic materials intended for orthopaedic implants. The report is an analytical summary of changes in the expression of cancer-related genes in human chondrocytes of normal and neoplastic phenotype. Cq values (quantification cycle values) obtained from qRT-PCR reactions (quantitative real-time polymerase chain reactions) were used to count Fc values (fold change values) for each gene. Differences in Fc values obtained for primary and cancer cells grown on the surface of medical steel AISI316L and titanium-aluminum-vanadium alloy Ti6Al4V were then analyzed by t-Student test. The results indicate that for cancer cells grown on the surfaces of both examined materials the fold change greater than 2, usually considered essential, was found for LUM gene involved in sarcoma induction. For FOS gene, also involved in sarcoma induction, the Fc value was also very close to 2 in the primary cells exposed to Ti6Al4V alloy. The remaining observed changes were rather subtle, although they cannot be omitted from further studies because differences in gene expression in primary and tumor cells grown on the same biomaterial were statistically significant in several cases. The compilation of qRT-PCR experiments carried out on primary and cancer cells in parallel allowed to identify possible future contraindications for patients with a genetic predisposition to cancer or with cancer history.

Keywords: *transcriptomics, qRT-PCR, gene expression, orthopaedic implants, cancer, chondrocytes*

[Engineering of Biomaterials 157 (2020) 15-19]

doi:10.34821/eng.biomat.157.2020.15-19

Introduction

Among a wide variety of biomaterials used for implantations, metals and their alloys remain high on the ranking lists of the most commonly used materials. The reason for this lies in their satisfying mechanical properties, second to none in comparison to other classes of biomaterials. In fact, it is only the matter of biocompatibility that may be the critical point for the selection of metals for some clinical applications [1,2]. Still a lot can be done to improve the biofunctionality and biocompatibility of metallic implants, especially through the effective methods of surface modifications. Laser surface modification is one of the most promising approaches to obtain high biocompatibility of metallic implants, which in the case of their orthopaedic applications mainly comes to induction of osteointegration processes [3].

There are numerous reports on the formation of cancer changes adjacent to the implant or in places distant but temporally correlated with the implantation. This phenomenon is strongly marked in dental implantology, where one of the main cancer types located in close proximity of dental implants is squamous cell carcinoma [4]. At the moment there is no indisputable data on the initiating of carcinogenesis by implants used in orthopaedics, although this subject has been often discussed in works in the last three decades. For example, after the total hip arthroplasty, the appearance of malignant neoplasms in the area of endoprostheses, including osteoma, osteosarcoma, lymphoma, or squamous cell carcinoma has been reported [5,6]. However, no mechanism is fully confirmed, and the issue of accelerated tumour induction at the implantation site is still poorly understood and unclear.

A literature review on clinical reports indicates that cancer changes situated in the bone and affecting not typically osteoblasts but chondrocytes and cartilage tissue may be the reason of failure in the orthopaedic implantation process [7]. What is more, some benign tumors like enchodroma, which are very often difficult to diagnose, can transform into chondrosarcoma over the years [8]. Combining all the above disturbing reports became the impetus for selecting cartilage tissue cells (primary chondrocytes and chondrosarcoma cells) to perform this study. The assumption of this work was to verify whether immortalized cell lines with neoplastic phenotype show an altered response to contact with implant material when compared to primary cell lines of the same type.

Transcriptomics techniques seem to be irreplaceable to thoroughly investigate this phenomenon. Methods enabling examining the changes in gene expression have gained popularity over the last decade and become the obvious choice to assess the materials biocompatibility at a molecular level [9,10]. In fact, the possibilities offered by these techniques are huge and can be underestimated. One of them - the qRT-PCR technique - was implemented in this work.

Materials and Methods

Cell cultures

Primary chondrocytes line HC-a derived from the human articular cartilage were purchased from ScienCell Research Laboratories (Cat. #4650), together with all the reagents necessary for the culture. The cells were cultured at 37°C and 5% CO_2 in Chondrocyte Medium (CM, Cat. #4651) supplemented with the fetal bovine serum (FBS, Cat. #0025), chondrocyte growth factors (CGS, Cat. #4682) and antibiotics (penicillin-streptomycin solution, Cat. #0503). The medium was changed every three days and the cells were subcultured at 95% confluency.

Secondary chondrocytes line SW 1353 derived from a patient with chondrosarcoma were from ATCC (ATCC-HTB-94). These cells were cultivated at 37°C in Leibovit'z L-15 Medium (ATCC, Cat. #30-2008) supplemented with the fetal bovine serum (Capricorn Scientific, Cat. #FBS-12A) and antibiotics (penicillin-streptomycin solution from ScienCell, Cat. #0503) in free gas exchange with atmospheric air.

Tested materials

The subject of this study were two types of metallic materials shaped as 16-mm diameter discs used for orthopaedic implant production. The metals are medical steel AISI 316L and titanium alloy Ti6Al4V. The materials surface was modified by grinding. Before each experiment, the samples were washed for 15 min in deionized water and for the next 15 min in 70% ethanol in an ultrasonic bath. Then the discs were sterilized with dry hot air.

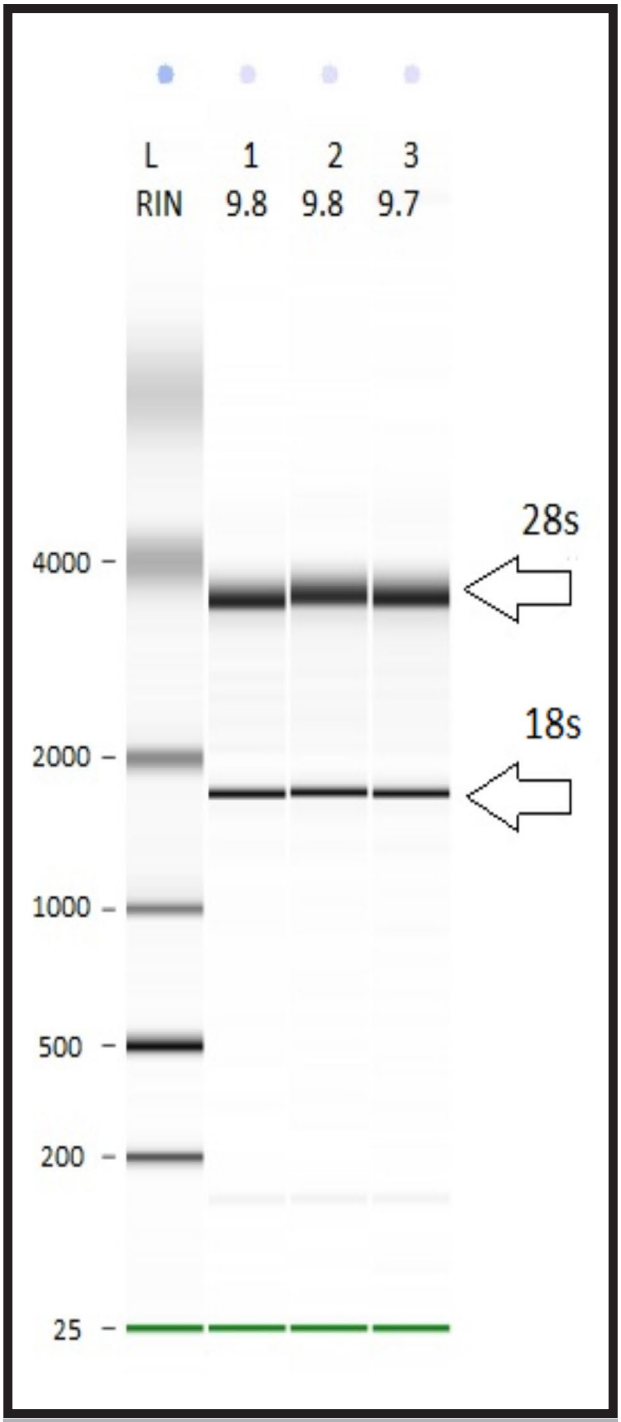

FIG. 1. Capillary electrophoresis carried out by Agilent's 2100 bioanalyzer for HC-a cells (L - ladder, 1 - control, 2 - AISI316L, 3 - Ti6Al4V). Two main ribosomal fractions (subunits 28s and 18s) are clearly marked. The RIN values (RNA integrity number) for all samples (1-3) close to 10 indicate perfect integrity of isolated material suitable for qRT-PCR.

RNA isolation and purification

For the RNA isolation experiment, the HC-a and SW 1353 cells were seeded on the surface of sterile samples placed in 12-well plates with the density of 100 000 cells/ml and incubated for 48 h in 37°C and 5% CO_2 atmosphere (HC-a) or without the additional CO_2 supply (SW 1353). The control was the cells grown on the surface of the standard well of a culture plate.

After the 48 h incubation the cells were harvested by trypsinization with 0.25% Trypsin-EDTA solution (ScienCell, Cat. #0103) and their quantity and viability were measured with trypan blue (ScienCell, Cat. #0203) in an automatic cell counter. Then the cells were transferred onto the system of columns from GeneMATRIX Universal RNA Purification Kit (EURx Ltd, Cat. #E3598) and the isolation and purification of total RNA was proceeded according to the procedure described in the manufacturer's protocol. In the next step, using Agilent's 2100 bioanalyzer, the quality and purity of isolated RNA were assessed by the means of capillary electrophoresis. An example image of the capillary electrophoresis performed for HC-a cells is presented in FIG. 1.

qRT-PCR reaction

Finally, the reverse transcription was performed with the use of the iScript cDNA Synthesis Kit (BIO-RAD, Cat. #1708891). The newly synthesized cDNA was used to carry out qRT-PCR reaction using the CFX96 Touch thermal cycler (BIO-RAD) and 2xSsoAdvanced Universal SYBR Green Supermix reagent (BIO-RAD, Cat. #1725274) on 96-well custom plates. The custom plates contained primers of 19 genes associated with the development of tumorigenic processes chosen basing on the literature review. The selected genes are listed in TABLE 1. GAPDH and AKTB were set as the reference genes.

The above experiment, from the seeding of cells, through the RNA isolation and purification, ending with the qRT-PCR reaction, was performed in seven independent repetitions for each cell line. The scheme of the standard gRT-PCR experiment is shown in FIG. 2.

Results and Discussions

A key parameter to analyze the gene expression changes via the qRT-PCR technique is the Cq value (quantification cycle value). Cq can be defined as a number of cycles after which the signal exceeds the detection threshold and, in fact, it is a measure of the gene expression. The Cq values obtained for every single gene from each repetition of the qRT-PCR reaction were analyzed using the comparative method, based on the Livak mathematical model. This method allows to calculate the relative difference of the expression level of a given gene between the test samples (RNA from the cells cultured on the biomaterials' surface) and control samples (RNA from the cells not stimulated by the presence of materials) [12].

GAPDH and AKTB were set as the reference genes. They were in constant expression in cells, yet at fluctuating levels. The difference between the Cq values of the qRT-PCR reaction running on the template of the test gene and the reference gene (ΔCq) was calculated for individual samples (test and control). Then, ΔΔCq (the difference between the ΔCq of the test and the ΔCq of the control sample) was indicated. Finally, the Fc value (fold change value) was calculated - the normalized value of the expression level of a given gene in the test sample in relation to the expression level of the same gene in the control sample ($Fc = 2^{-\Delta\Delta Cq}$). For the purposes of the analysis, it was assumed that $Fc \geq 2$ ($\log_2 Fc \geq 1$) means gene overexpression, while $Fc \leq 0.5$ ($\log_2 Fc \leq -1$) may be interpreted as gene suppression [12,13].

TABLE 1. 19 genes promoting cancer formation selected for the experiment to design a custom PCR plate [11].

Gene symbol		Name of encoded protein	Which process the gene regulates?
1.	BCL2	apoptosis regulator Bcl-2	negative apoptosis regulation
2.	CASP3	caspase-3	
3.	ABL1	tyrosine-protein kinase ABL1	
4.	BAK	Bcl-2 homologous antagonist/killer	positive apoptosis regulation
5.	TNF	tumor necrosis factor	
6.	RB1	retinoblastoma-associated protein	cell cycle
7.	CHEK2	checkpoint kinase 2	
8.	VEGFa	vascular endothelial growth factor A	angiogenesis
9.	ABCB1	multidrug resistance protein 1	drug resistance
10.	ATM	serine-protein kinase ATM	
11.	CDKN1A	cyclin-dependent kinase inhibitor 1	
12.	NFKB1	DNA-binding factor KBF1	transcription
13.	JUN	transcription factor AP-1	
14.	TRF1	telomeric repeat-binding factor 1	cell aging
15.	PINX1	PIN2/TERF1-interacting telomerase inhibitor 1	
16.	MMP1	matrix metalloproteinase-1	proteolysis
17.	LUM	lumican - keratan sulfate proteoglycan lumican	sarcoma induction
18.	FOS	proto-oncogene c-Fos	
19.	NOS-2	nitric oxide synthase	hypoxia

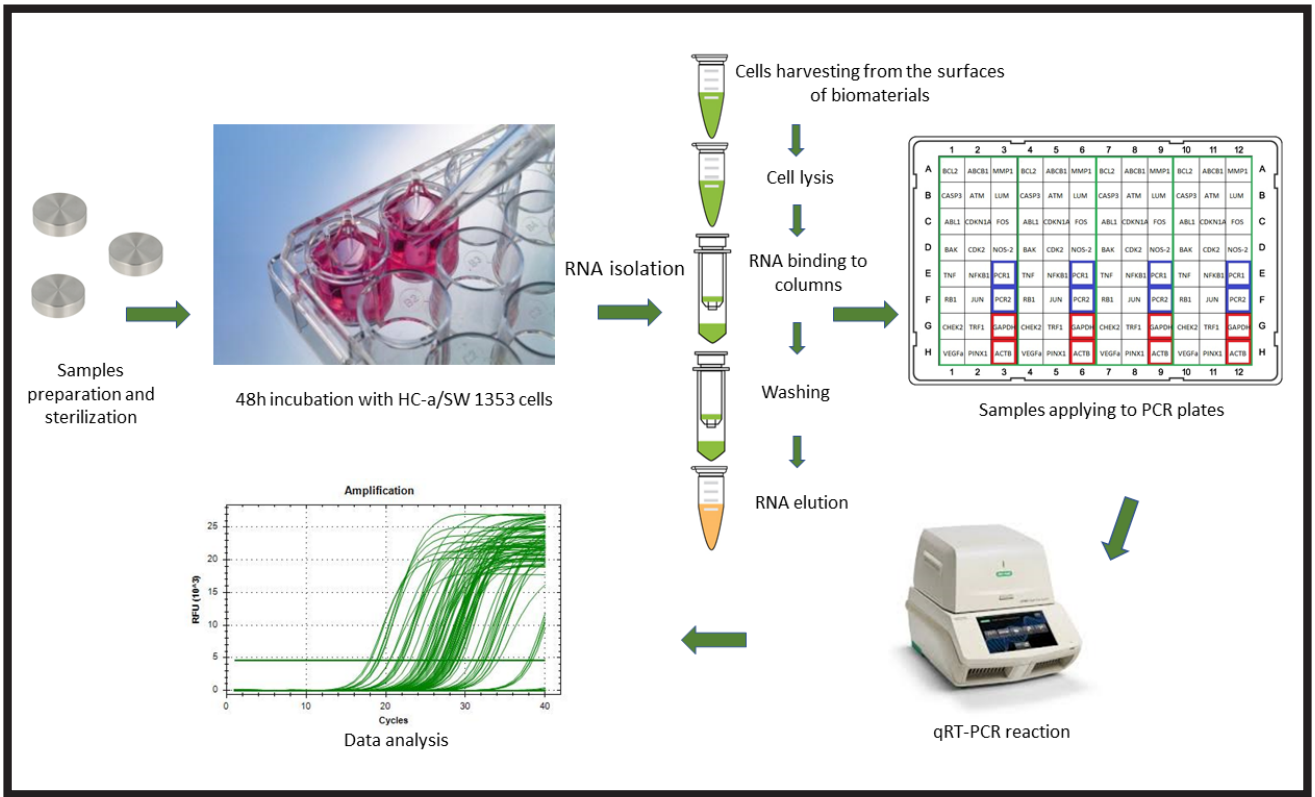

FIG. 2. The scheme of the standard qRT-PCR experiment: starting with sample preparation, through RNA isolation and purification, ending with qRT-PCR reaction.

Below, the graphs present mean values of log_2Fc obtained from seven independently performed qRT-PCR reactions for each examined gene and for both tested materials. The mean values are given with standard deviations (FIGs 3 and 4).

The t-Student test was used for the statistical analysis of Fc values of each gene in the primary and neoplastic chondrocytes grown on the examined surfaces (AISI 316L and Ti6Al4V). The results of statistical analysis are marked in FIGs 3 and 4 (VS - very significant, S - significant, MS - marginally significant).

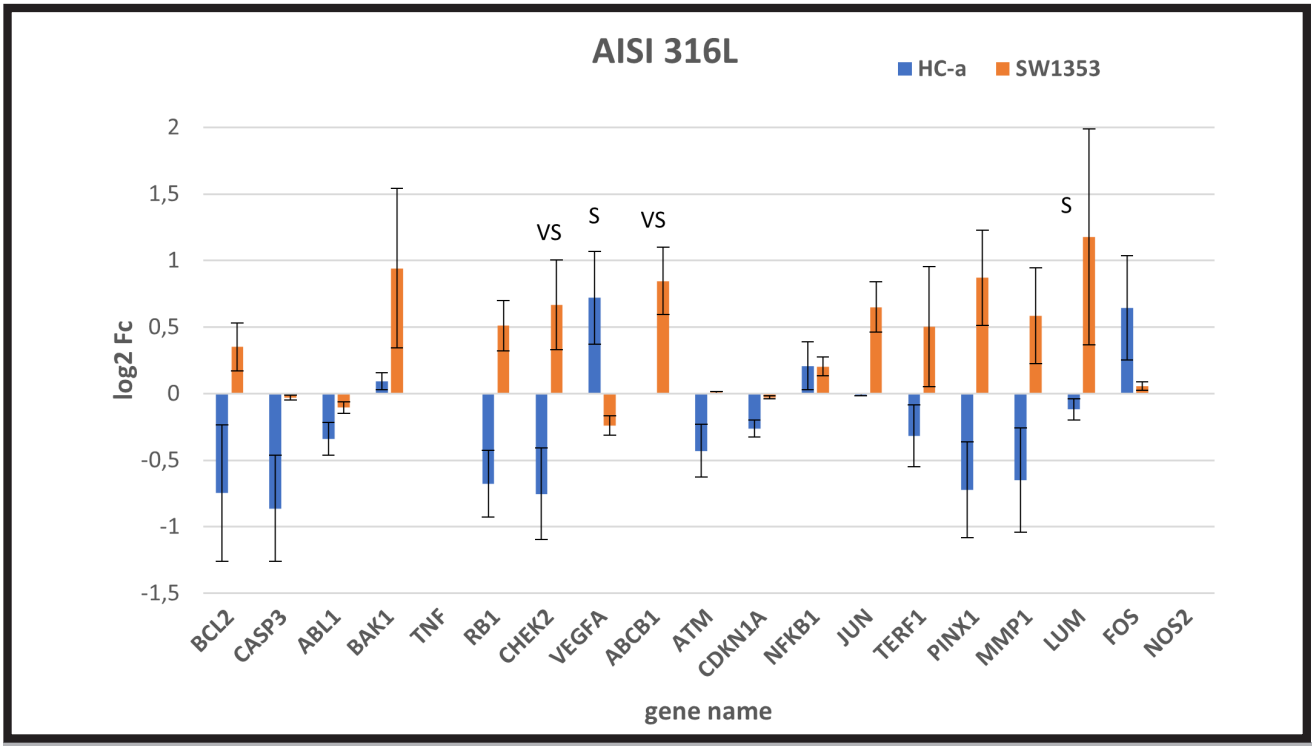

FIG. 3. The mean values of expression changes of individual genes expressed as log_2Fc and standard deviations obtained from 7 qRT-PCR reactions for HC-a and SW1353 chondrocytes grown on the surface of medical steel AISI 316L with statistical significance (MS - marginally significant for $p < 0.07$, S - significant for $p < 0.05$, VS - very significant for $p < 0.005$).

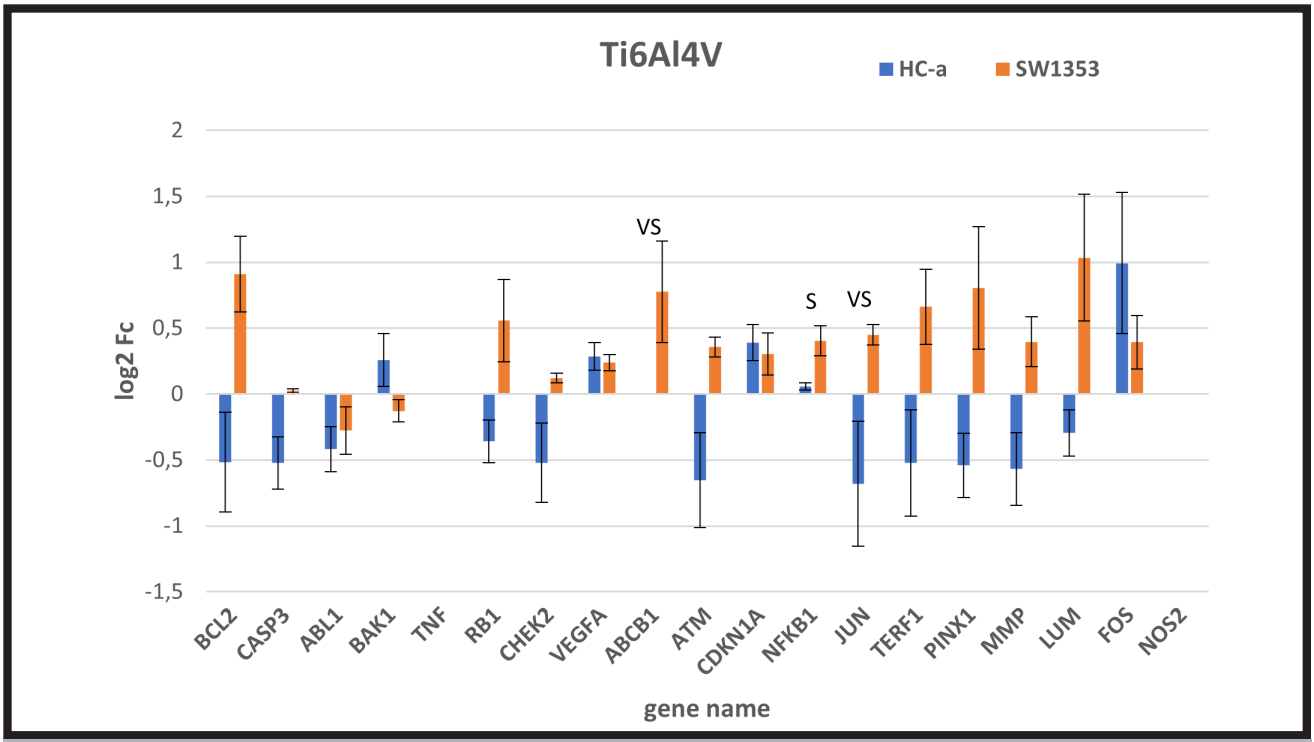

FIG. 4. The mean values of expression changes of individual genes expressed as log_2Fc and standard deviations obtained from 7 qRT-PCR reactions for HC-a and SW1353 chondrocytes grown on the surface of Ti6Al4V alloy with statistical significance (S - significant for $p < 0.05$, VS - very significant for $p < 0.005$).

Out of the 19 examined genes, the changes in gene expression were observed for 16 and 17 of them, for the HC-a and SW1353 cells, respectively. In both cell lines two genes – TNF and NOS-2 – were not expressed at all for any of the tested materials. TNF gene is responsible for positive apoptosis regulation, whereas NOS-2 – for the process of hypoxia. Another gene, ABCB1 gene, coding the multi-drug resistance protein that participates in failures in many different therapies, was active only in chondrosarcoma cells, not in primary ones. This confirms the well-known phenomenon of the tumor cell resistance to pharmacological treatment [14].

The predominant direction of changes for HC-a cells was the gene suppression (negative values of $\log_2$Fc), whereas for SW1353 tumor chondrocytes the direction of changes was exactly opposite, and in most cases, the gene overexpression could be observed (positive values of $\log_2$Fc). However, out of all examined genes for both cell lines and both types of the tested materials only one gene – LUM – was properly overexpressed according to the assumptions of this analysis, i.e. only this gene reached the value of $\log_2$Fc greater than 1. This situation was observed only in two cases – for the SW1353 cells after contact with AISI316L and Ti6Al4V. The LUM gene codes the proteins related with degradation of extracellular matrix and keratin metabolism. In this way, they may limit the tumor progression by preventing extracellular matrix collagen proteolysis. In cancer cells, these proteins are usually down-regulated. The LUM gene overexpression in cancer chondrocyte cells was statistically significant in comparison to the primary chondrocytes (very significant difference for AISI316L and Ti6Al4V). The results of the experiments may suggest that these two materials tend to limit tumor growth [15]. It is also worth paying attention to the FOS gene, for which the Fc value is very close to 2 in HC-a primary cells grown on the surface of the Ti6Al4V alloy. This gene encodes the c-Fos protein which is the human homologue of retroviral oncogene v-Fos and has an oncogenic activity [16].

The remaining observed differences in the expression of individual genes in primary and neoplastic cells are not so spectacular, but even these subtle differences should be taken into account in further research. Certainly, the number of genes examined in this study is not enough to draw far-reaching conclusions, it was only a starting point to find some possible tendencies. Gaining more knowledge in this area requires further intensive research, the results of which may be of paramount importance in choosing a safe biomaterial, especially for patients with a cancer history.

Conclusions

The analysis of changes in the expression of cancer-related genes is the most accurate approach to assess the risk of implants inducing or intensifying carcinogenesis. The compilation of qRT-PCR experiments carried out on primary and cancer cells in parallel allowed to identify possible future contraindications for patients with a genetic predisposition to cancer or with cancer history. What is more, this approach may be a crucial step to select the right biomaterial for a specific patient, which is the goal of personalized medicine.

Acknowledgements

This work has been supported by the National Centre for Research and Development, project number POIR.04.01.04-00-0058/17-00 "Projektowanie i wytwarzanie spersonalizowanych implantów medycznych" Custom-ITAP.

ORCID iD

M. Walkowiak-Przybyło:
https://orcid.org/0000-0002-2162-9858

References

[1] Kaur M., Singh K.: Review on titanium and titanium based alloys as biomaterials for orthopaedic applications. Mater Sci Eng C Mater Biol Appl. 102 (2019) 844-862.
[2] Gotman I.: Characteristics of metals used in implants. J Endourol. 11(6) (1997) 383-389.
[3] Chenchen W., Hongxing H., Zhipeng L., Yifan S., Yong X., Gangqiang Z., Xiangqiong Z., Jun D., Shichang Z., Tianhui R., Yadong Z.: Enhanced Osseointegration of Titanium Alloy Implants with Laser Microgrooved Surfaces and Graphene Oxide Coating. ACS Appl Mater Interfaces 11(43) (2019) 39470-39483.
[4] Jeelani S., Rajkumar E. et al.: Squamous cell carcinoma and dental implants: A systematic review of case reports. J Pharm Bioallied Sci. 7(2) (2015) S378–S380.
[5] Smith A.J., Dieppe P. et al.: Risk of cancer in first seven years after metal-on-metal hip replacement compared with other bearings and general population: linkage study between the National Joint Registry of England and Wales and hospital episode statistics. BMJ (2012) 344.
[6] Levasic V., Milosev I. et al.: Risk of cancer after primary total hip replacement: The influence of bearings, cementation and the material of the stem. Acta Orthop. 89(2) (2018) 234–239.
[7] Mustaki L., Goetti P., Gallusser N., Morattel B., Rüdiger H., Cherix S.: Unrecognized Chondrosarcoma as a Cause of Total Hip Arthroplasty Failure. Arthroplast Today 7 (2021) 84-90.
[8] Herget G.W., Strohm P., Rottenburger C., Kontny U., Krauß T., Bohm J., Sudkamp N., Uhl M.: Insights into Enchondroma, Enchondromatosis and the risk of secondary Chondrosarcoma. Review of the literature with an emphasis on the clinical behaviour, radiology, malignant transformation and the follow up. Neoplasma 61(4) (2014) 365-378.
[9] Komorowski P., Siatkowska M., Kamińska M., Jakubowski W., Walczyńska M., Walkowiak-Przybyło M., Szymański W., Piersa K., Wielowski P., Sokołowska P., Białkowska K., Makowski K., Elgalal M., Kierzkowska A., Ciupik L., Walkowiak B.: Comprehensive Biological Evaluation of Biomaterials Used in Spinal and Orthopedic Surgery. Materials (Basel).13(21) (2020) 4769.
[10] Wang X., Xia Y., Liu L., Liu M., Gu N., Guang H., Zhang F.: Comparison of MTT assay, flow cytometry, and RT-PCR in the evaluation of cytotoxicity of five prosthodontic materials. J Biomed Mater Res B Appl Biomater. 95(2) (2010) 357-364.
[11] www.genecard.org
[12] Livak K.J., Schmittgen TD.: Analysis of relative gene expression data using real-time quantitative PCR and the 2(-Delta Delta C(T)) method. Methods. 25(4) (2001) 402-408.
[13] Bustin S.A., Benes V., Garson J.A. et al: The MIQE guidelines: minimum information for publication of quantitative real-time PCR experiments. Clin Chem 55(4) (2009) 611-622.
[14] Rueff J., Rodrigues A.S.: Cancer Drug Resistance: A Brief Overview from a Genetic Viewpoint. In: Rueff J., Rodrigues A. Cancer Drug Resistance. Methods in Molecular Biology. 1395 (2016) 1-18. Humana Press, New York.
[15] Pietraszek K., Chatron-Colliet A., Brézillon S., Perreau C., Jakubiak-Augustyn A., Krotkiewski H., Maquart F.X., Wegrowski Y.: Lumican: a new inhibitor of matrix metalloproteinase-14 activity. FEBS Letters. 588 (23) (2014) 4319–4324.
[16] Milde-Langosch K.: The Fos family of transcription factors and their role in tumourigenesis. Eur. J.Cancer. 41 (16) (2005) 2449–2461.

LONG-TERM MECHANICAL TESTING OF MULTIFUNCTIONAL COMPOSITE FIXATION MINIPLATES

Karol Gryń*

AGH University of Science and Technology,
Faculty of Materials Science and Ceramics,
Department of Biomaterials and Composites,
Al. Mickiewicza 30, 30-059 Krakow, Poland
*e-mail: kgryn@agh.edu.pl

Abstract

This paper presents the analysis and comparison of the results of mechanical testing of dumbbell-shaped specimens and multifunctional fixation miniplates made via injection forming. Three types of materials were used: a) polylactic acid; b) a composite made of a polylactic acid matrix modified with tricalcium phosphate β-TCP; c) a composite made of a polylactic acid matrix modified with a mixture of bioceramic powders of tricalcium phosphate β-TCP and hydroxyapatite HAp. All the samples were stored in normal conditions, no special treatment was applied. Tests were conducted right after samples were prepared and they were repeated two and four years after preparation. The values of basic mechanical parameters and stress-strain curves were recorded and analyzed. The attention was focused on changes in time of tensile strength and stiffness of materials and implants. It was discovered that having been stored for four years in the open air, without sunlight, with no hermetic sealing, and no sterilization, all the materials (PL38, PL38/TCP, PL38/TCP/HAp) showed slight changes in mechanical characteristics when compared to the data of the initial samples tested after fabrication. These changes were not critical and did not adversely affect either tensile strength or Young's modulus of the implants. All the analyzed miniplates maintained their mechanical properties at an acceptable level, fulfilling requirements for fixation devices for osteosynthesis. Therefore, it was proposed that the expiry date of these implants can be indirectly determined, based on long-term mechanical testing.

Keywords: *multifunctional composites, fixation plates, mechanical testing, implant expiry date, polylactide acid, calcium-phosphate ceramics*

[Engineering of Biomaterials 157 (2020) 20-25]

doi:10.34821/eng.biomat.157.2020.20-25

Introduction

In recent years the development and application of new composite materials for the production of implants have become one of the main topics in the field of biomaterials. The introduction of modifiers into polymeric matrices to improve their strength or increase their stiffness is already a standard procedure [1,2]. There are numerous laboratories around the world where scientists try to provide novel materials with additional therapeutic features and functions. Among them, there are the Department of Biomaterials and Composites (Faculty of Materials Science and Ceramics of the AGH University of Science and Technology in Krakow) and MEDGAL Ltd. (Białystok, Poland). The key achievement of this cooperation were multifunctional composite biomaterials designed to manufacture biodegradable fixation miniplates. These new composite implants made of PLA modified with bioactive ceramic powders (β-TCP and HAp) not only ensure mechanical stability of bone fragments but also support local healing processes and intensify processes of reconstruction of the damaged bone tissue [3].

Besides the standard material and biological description, the most important issues that the manufacturer is obliged to determine are time and conditions of storing the product and its expiry date. In Poland, there are no legal regulations and precise requirements or procedures to determine the usefulness of medical devices, implants or medical equipment. It is generally accepted that the expiry date of reusable products is determined by the quality of packaging and sterilization processes. Thus, it guarantees that the product is safe and sterile until the moment of application. In other words, the expiry date is related exclusively to the biological purity and sterility of the product [4]. Materials commonly used in medicine e.g. metals, alloys or biostable polymers can be treated as reusable products and in these cases "the sterility principle" may be applied. However, the question arises with regard to degradable materials. In most cases, such materials are multiphase systems made of resorbable polymer matrices modified with various additives (drugs, bioactive ceramics, etc.). That is why the variety of possible reactions affecting the final properties of the implants' material may occur [5-10]. A series of complicated, laborious, and expensive structural studies must be performed to assess the behaviour of these materials in time. However, is it necessary in all cases? Is there any other way to verify this behaviour? Based on the presented research results, an inexpensive alternative to estimate the expiry date of an implant is proposed. It is the long-term data obtained through mechanical testing.

Materials and Methods

The samples were made from three types of materials: a) PURASORB PL38 poly(lactic acid), an amorphous resorbable polymer with Food and Drug Administration (FDA) approval for medical applications (PURAC, Europe); b) a composite of the PURASORB PL38 resorbable matrix modified with 8vol% micrometric β-TCP tricalcium phosphate powder (Chema Elektromet, Poland); c) a composite of the resorbable PURASORB PL38 matrix modified with two types of bioceramic additives; total volume fraction did not exceed 8vol%: micrometric tricalcium phosphate powder β-TCP ~7.5vol% and nanometric hydroxyapatite powder HAp ~0.5vol% (Chema Elektromet, Poland).

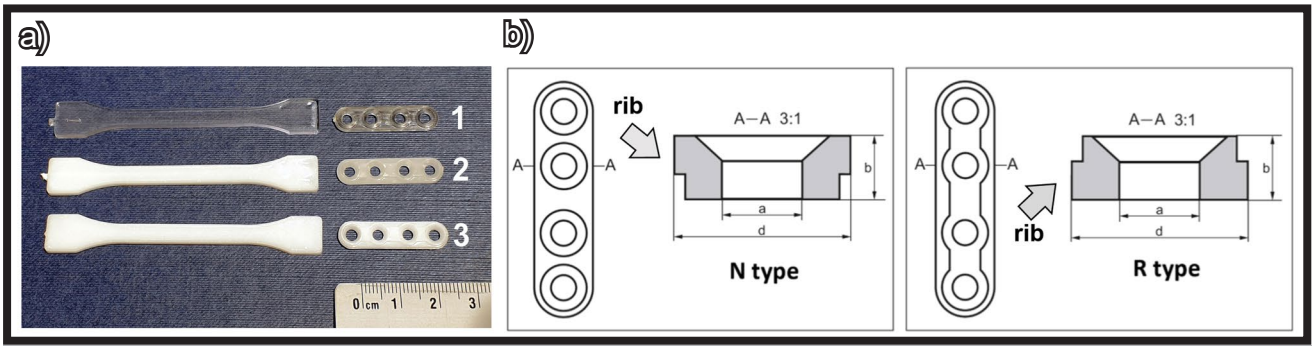

FIG. 1. a) Examples of dumbbell-shaped specimens and fixation miniplates used for testing. 1 - PL38; 2 - PL38/TCP; 3 - PL38/TCP/HAp; b) Schematic sketches of the I-shaped four-hole miniplate: type "N" with reinforcing rib from the bottom; type "R" with reinforcing rib from the top.

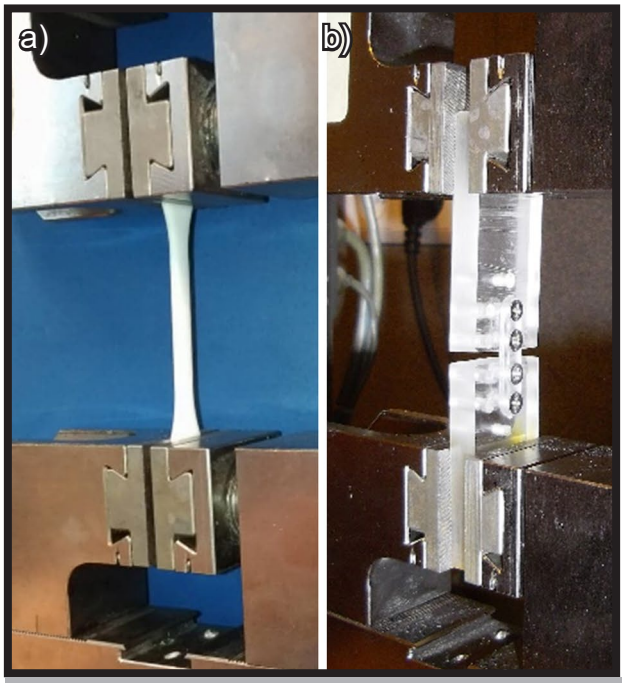

FIG. 2. a) Dumbbell-shaped specimen mounted and ready for testing; b) Simulated model of osteosynthesis with fixation miniplate.

Both powders were approved for medical applications. The samples were made by injection molding on a vertical screw-piston injection molding machine (Multiplas V4-S-15N, Taiwan) at the processing temperature of 180°C, and the pressure in the injection system of 90 kg/cm^2 (~9.0 MPa). Two types of the samples were produced: a) dumbbell-shaped specimens (length: 75 mm, width: 5 mm, thickness: 2 mm) (FIG. 1a); b) I-shaped four-hole miniplates with length: 29 mm, width: 7 mm, thickness: 2 mm, hole diameter: 3 mm (FIG. 1a). Two geometric variants of miniplates were prepared: with a reinforcing rib on the lower surface (type "N"); with a reinforcing rib on the upper surface (type "R") (FIG. 1b). The detailed descriptions of the preparation of dumbbell-shaped specimens and fixation miniplates along with the results from the preliminary tests conducted in 2014-2015 were published in the article: "Mechanical characterization of multifunctional resorbable composite plate for osteosynthesis" [3]. All samples were stored at room temperature, isolated from sunlight. The samples were not sterilized or hermetically sealed. For each type of the samples: dumbbell-shaped, "N" type miniplates and "R" type miniplates, five specimens were examined in the beggining of the experiment, and after two and four years.

All specimens were tested under the same loading scheme and conditions. The static uniaxial tensile tests were performed in accordance with the PN-EN ISO 527-1: 2012 standard. The research was carried out on Zwick 1435 testing machine, coupled with TestExpert v8.1 software. The traverse speed was set at 2 mm/min. The dumbbell-shaped specimens were tested in standard clamps (FIG. 2a). The I-shaped four-hole fixation miniplates were tested in a model simulating osteosynthesis: two blocks of plexiglass (PMMA) measuring 50x25x8 mm were cut. The fixation miniplates were mounted on the blocks using stainless steel screws with nuts (M2.5 A4-70). The gap between the PMMA blocks simulating a bone fracture measured 2 mm in width (FIG. 2b). Screws were tightened with tightening torque M_d = 20 cNm (± 0.01 cNm) with a digital torque wrench (POLTORQUE BMS-150). The values of tensile strength R_m and Young's modulus E were determined. The sets of $\sigma = f(\varepsilon)$ curves were obtained. Additionally, the damaged specimens underwent microscopic examination regarding the fractures.

Results and Discussion

Dumbbell-shaped specimens

When analyzing tensile curves for the dumbbell-shaped specimens (FIG. 3), all the PL38 samples revealed a certain range of plastic deformation. The widest range was observed for the initial specimens (tested right after manufacturing). The local plastic deformation was confirmed during microscopic observations. There was a whitening area around the line of fracture and the small "necking" was found (FIG. 4a). For the composite samples PL38/TCP and PL38/TCP/HAp, the deformation had the elastic-brittle character. For all the materials and all the time intervals, the dumbbell-shaped specimen fracture was located at ~1/5 of the length of the measurement base. The crack line was perpendicular to the long axis of the specimen and the fracture was flat-parallel. Almost no plastic deformation on the tensile curves was recorded, therefore it can be concluded that the composite fracture was brittle (FIG. 4b, 4c).

The comparison of dumbbell-shaped specimens revealed no significant changes in the tensile strength values recorded in time (FIG. 5). For the PL38/TCP/HAp composite, a slight strengthening effect was observed: after 2 years by about 8% and after 4 years by about 10%.

In general, the materials stiffness increased with time (FIG. 5). The biggest changes were recorded for PL38 – for instance, its Young's modulus almost doubled after four years of storage. For the PL38/TCP/HAp composite there were not such significant differences in the value of Young's modulus: less than 20%.

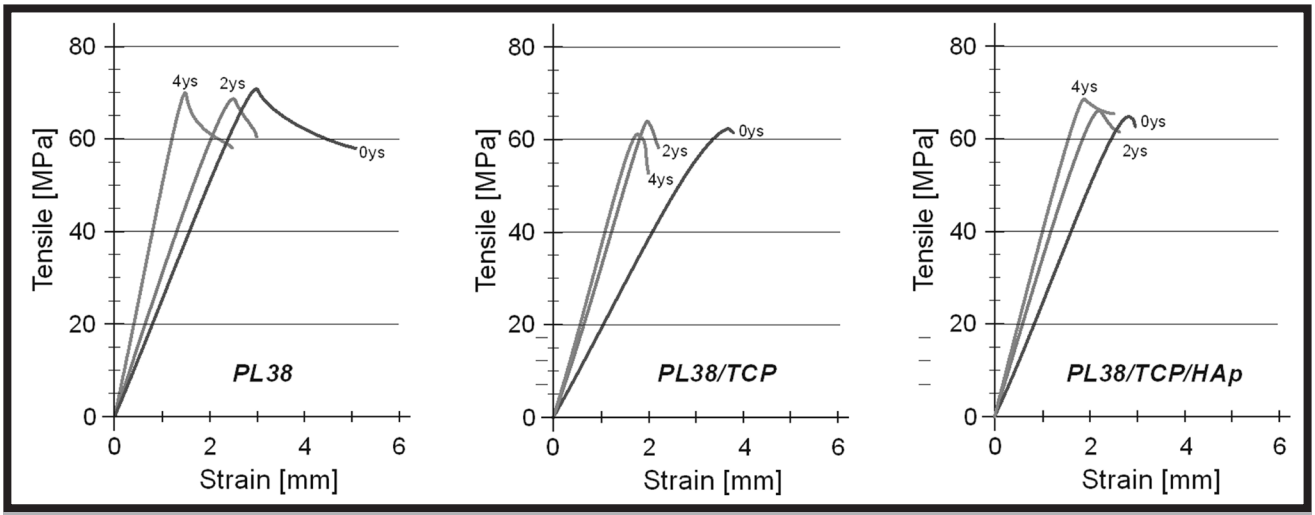

FIG. 3. Examples of tensile curves of dumbbell-shaped specimens.
0ys - initial samples; 2ys - tested after two years; 4ys - tested after four years.

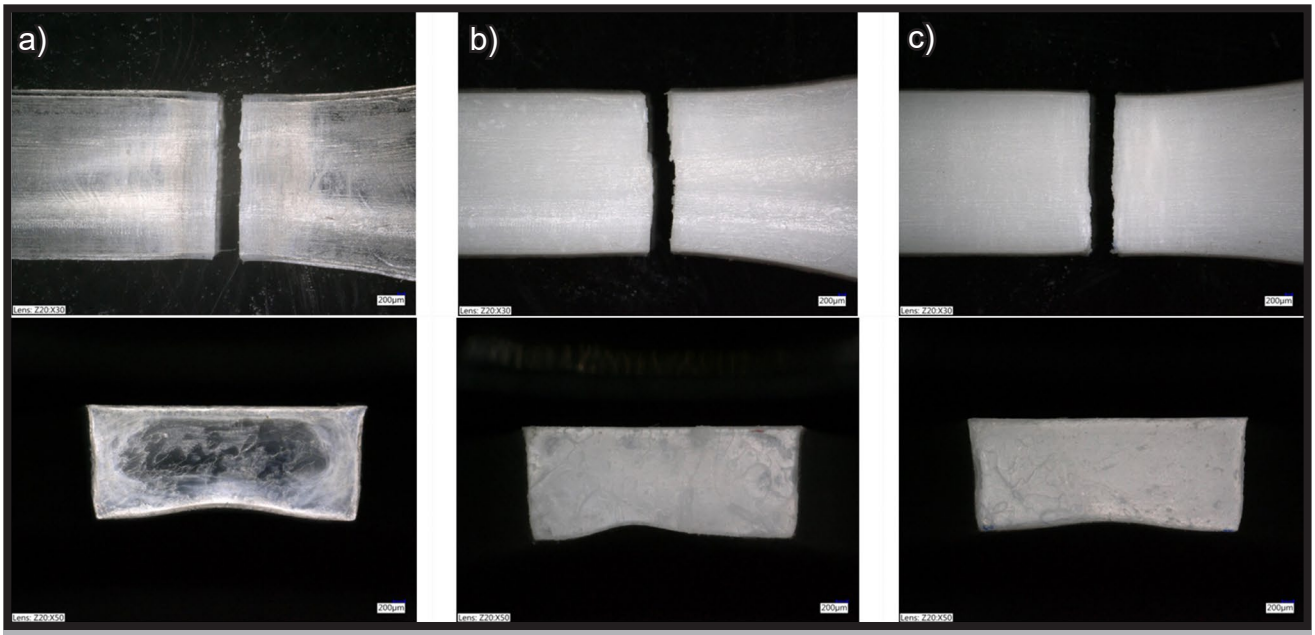

FIG. 4. Example of microscopic images of sample fracture (KEYENCE VHX-500, mag. x30; x50): a) PL38; b) PL38/TCP; c) PL38/TCP/HAp.

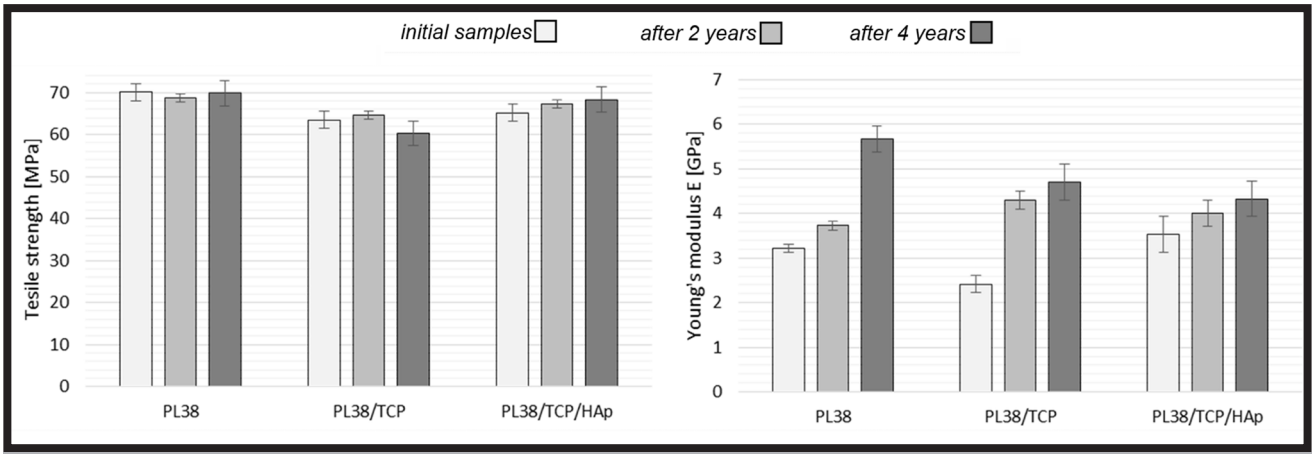

FIG. 5. Comparison of average R_m and E values obtained during mechanical testing of dumbbell-shaped specimens of the initial samples, after 2 and after 4 years.

Fixation miniplates

The results of the mechanical tests of the fixation miniplates are presented as tensile curves (FIGs. 6, 7) and graphic bars (FIGs. 8, 9).

All the curves show the tensile stress values fluctuation area and a subsequent decrease in the graph angle with respect to the strain axis. This might result from localized plastic deformation in the critical cross-section – i.e. the area of the fixation hole – causing changes in the implant geometry. The miniplate thickness might have decreased and the shape of the fixation hole changed from round to elliptic. Thus, the stress state ensuing from the pressure under the fixation screw conical head was no longer uniform. Nevertheless, it was also found that fixation miniplates with the reinforcing rib on the upper surface ("R" type) had better and more stable characteristics. The mechanical properties of the PL38 and PL38/TCP miniplates decreased with time. An interesting phenomenon was observed for the PL38/TCP "N" sample. After two years of storage, the tensile strength dropped by ~45% but after the next two years, it increased again. In the case of the PL38/TCP/HAp miniplates, different behaviour was noted. The longer the samples were stored, the higher tensile strength values were recorded. After two years the stiffness and Young's modulus values significantly increased but after the next two years they slightly decreased. It can be speculated that such behaviour could result from a change in the polymer crystallinity degree. It may also happen when moisture from the environment is absorbed, possibly due to the presence of HAp in the matrix. To confirm this hypothesis, additional structural tests and analysis are necessary.

In general, the obtained values of tensile strength for all types of miniplates were in the range of 35-65 MPa and the materials stiffness expressed by Young's modulus values fluctuated in the range of 7-14 GPa. Regardless of the storage time, the tested fixation miniplates match the characteristics of natural bone, as the bone tensile strength is 1-180 MPa, depending on the type (spongy/bony) and Young's modulus is from 0.007 GPa to 30 GPa [10].

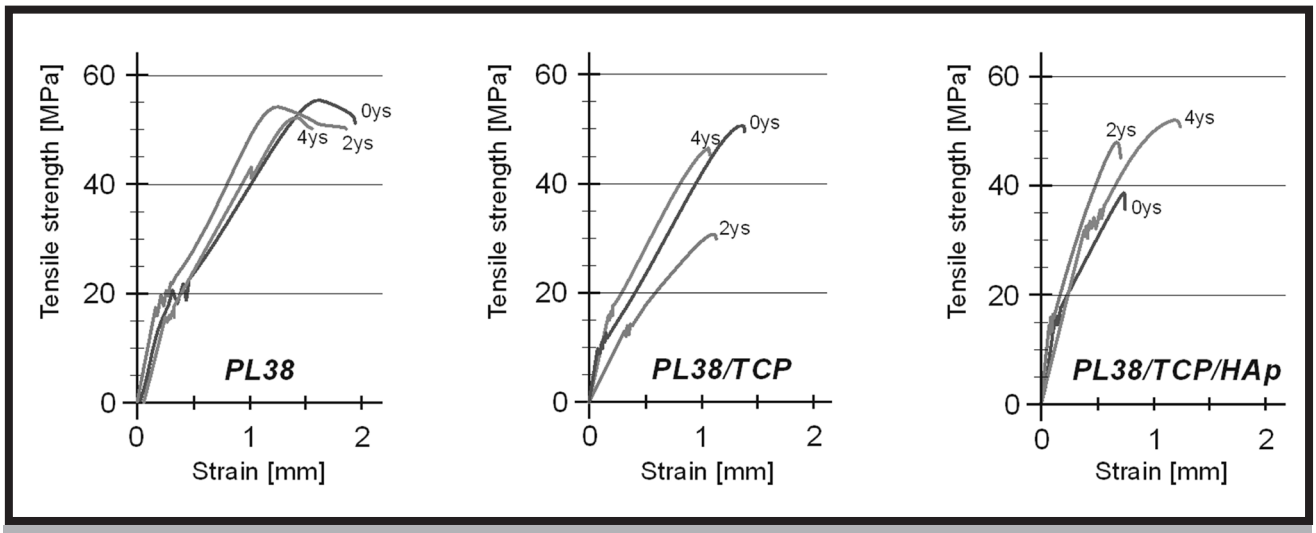

FIG. 6. Example tensile curves of "N" type miniplates.
0ys - initial samples; 2ys - tested after two years; 4ys - tested after four years.

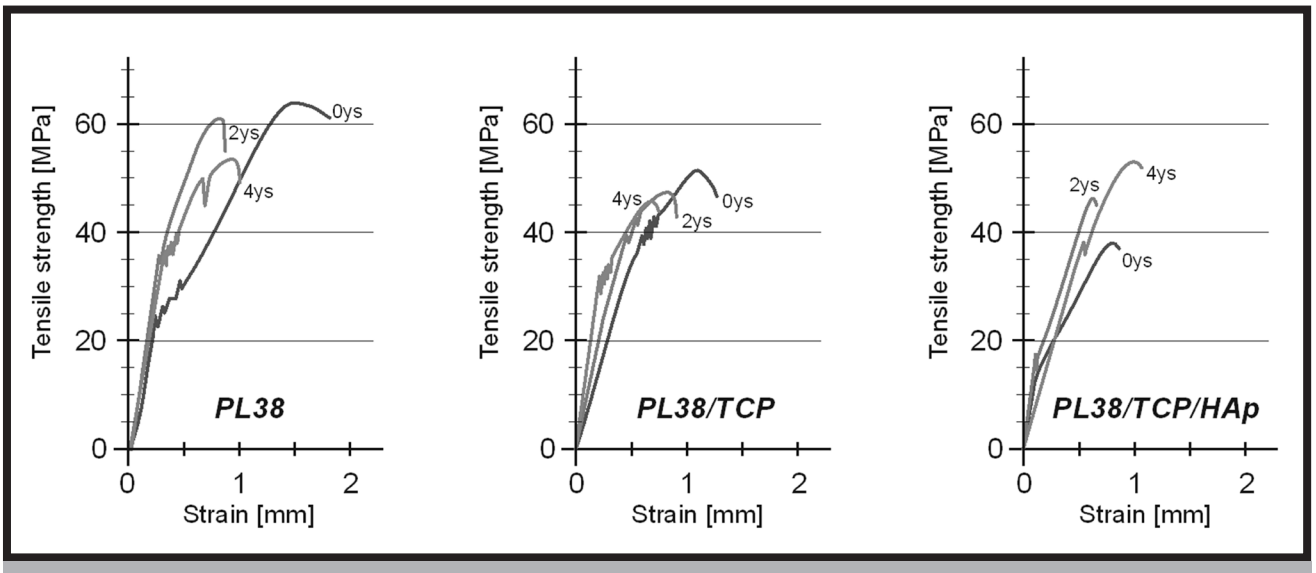

FIG. 7. Example tensile curves of "R" type miniplates.
0ys - initial samples; 2ys - tested after two years; 4ys - tested after four years.

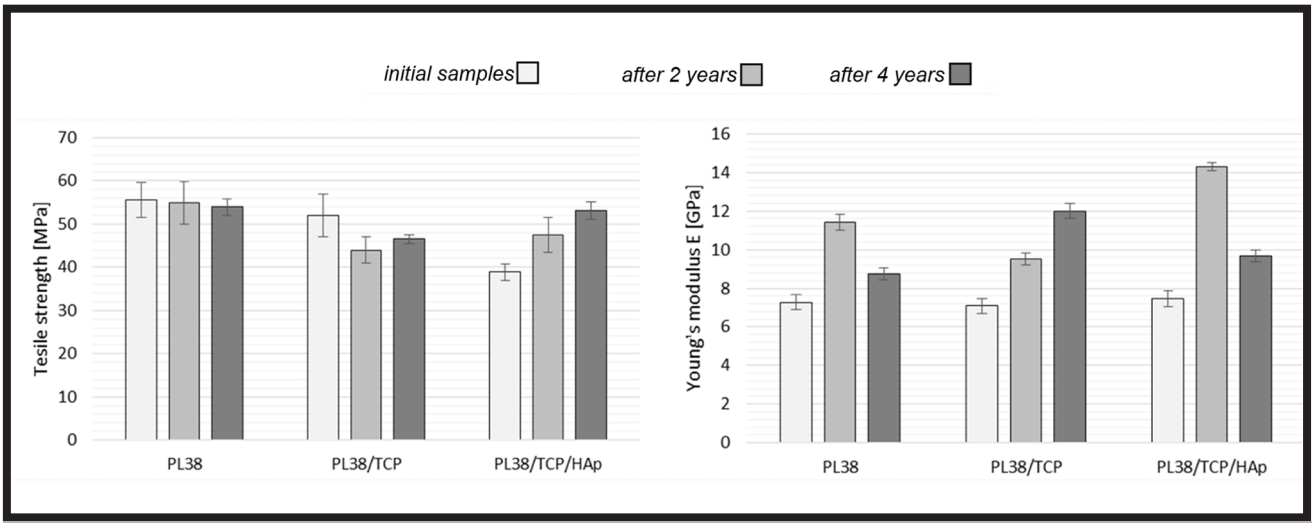

FIG. 8. Comparison of mechanical test results (R_m and E) of the "N" type fixation miniplates of the initial samples, after 2 and after 4 years.

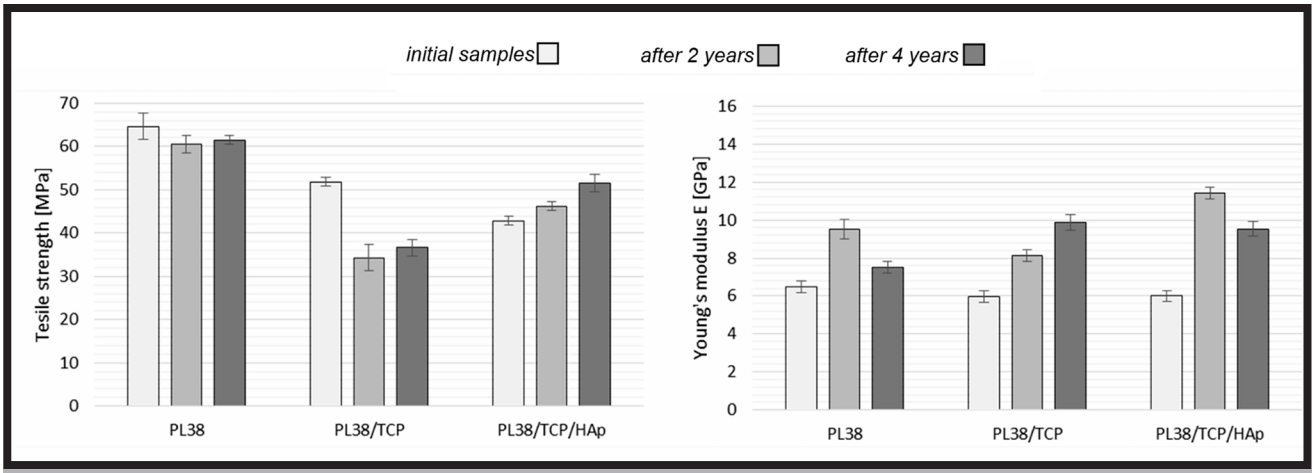

FIG. 9. Comparison of mechanical test results (R_m and E) of the "R" type fixation miniplates of the initial samples, after 2 and after 4 years.

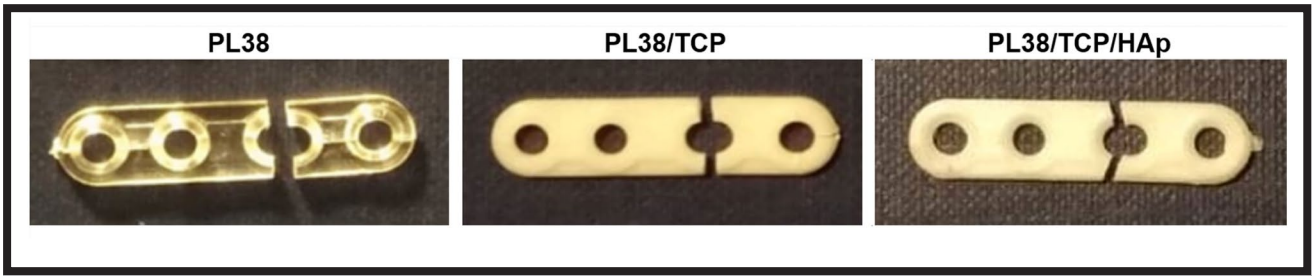

FIG. 10. Examples of miniplates after the mechanical testing. The characteristic manner of fracture can be seen.

The microscopic observation of the damaged fixation I-shaped four-hole miniplates revealed that both "R" and "N" type miniplates fractured in a predictable manner. The fractures occurred close to the first hole proximal to the centre of the miniplate (FIG. 10). The fracture was perpendicular or nearly perpendicular to the plane of tension and the crack was in the first critical cross-section (the weakest part of a miniplate). In the case of PL38, regardless of the storage time, a slight opacity of the specimen was observed in the fracture vicinity. This may indicate a slight local plastic deformation.

Due to the white colour and lack of transparency of the PL38/TCP and PL38/TCP/HAp composite miniplates, a similar analysis could not be performed. The fracture lines were in both cases straight and the crack was brittle. This characteristic brittle behaviour was also visible in the stress-strain curves.

Conclusions

Having analyzed the results of the tests, it can be concluded that all the materials (PL38, PL38/TCP, PL38/TCP/HAp) after four years of storage in the open air, without exposition to the sunlight, with no hermetic sealing, and no sterilization, showed slight changes in mechanical characteristics when compared to the data of initial samples tested after their fabrication. These changes might result from the degradation processes of the tested materials (e.g. absorption of moisture from the air, temperature changes). Nevertheless, these changes were not critical and did not affect negatively either the tensile strength or the implants stiffness. All the miniplates maintained their mechanical properties at an acceptable level. Therefore, it can be concluded that even after four years of storage they can be used as a fully valuable product. Considering its tensile strength and Young's modulus, even the weakest miniplate remained within the range required for materials used in osteosynthesis.

In conclusion, the presented methodology can be used to indirectly estimate the expiry date of composite implants. For two years the implant can be safely stored and used in surgery. Since its mechanical properties fulfil the requirements for osteosynthesis fixation device, the implant will surely perform its function properly during this period of time. However, the behaviour of such an "old" implant in the living organism is difficult to predict. Therefore, further studies, especially in a simulated biological environment and the *in vivo* tests will be necessary to verify the results of this work.

Acknowledgements

The study was performed in collaboration with MEDGAL Company within the R&D project: "Elaboration and implementation of the production technology of innovative bone implants made of polymer composites" (POIG.01.04.00-20-003/10).

ORCID iD

K. Gryń: https://orcid.org/0000-0001-6499-2465

References

[1] Marciniak J., Błażewicz S.: Biomateriały, Tom 4, Akademicka Oficyna Wydawnicza Exit, 2016

[2] Lincoln R.L., Scarpa F., Ting V.P., Trask R.S.: Multifunctional composites: a metamaterial perspective. Multifunct. Mater. 2 (2019) 043001.

[3] Gryń K., Szaraniec B., Morawska-Chochół A., Chłopek J.: Mechanical characterization of multifunctional resorbable composite plate for osteosynthesis. Engineering of Biomaterials 133 (2015) 22-33.

[4] Kudzia-Karwowska D.: Czynniki warunkujące okres przydatności wyrobów medycznych. Technika i technologia. Ogólnopolski Przegląd Medyczny 11 (2013) 15-17.

[5] Elsawy M.A., Ki-Hyun K., Akash J.W., Deep A.: Hydrolytic degradation of polylactic acid (PLA) and its composites. Renewable and Sustainable Energy Reviews 79 (2017) 1346-1352.

[6] Kulkarni A., Dasari H.: Current Status of Methods Used In Degradation of Polymers: A Review, MATEC Web of Conferences 144, 02023 (2018).

[7] Rivaton A., Gardette J.L., Mailhot-Jensen B.: Basic Aspects of Polymer Degradation, Macromol. Symp. 225 (2005) 129-146.

[8] Szaraniec B., Gryń K., Szponder T., Żylińska B.: Biodegradable fixation plates for veterinary medicine. Engineering of Biomaterials 125 (2014) 30-36.

[9] dos Santos V., Brandalise R.N., Savaris M.: Engineering of Biomaterials, Springer International Publishing 2017, ISBN 978-3-319-58607-6.

[10] Yuehuei H., Rob. Draughn R.: Mechanical Testing of Bone and the Bone-Implant Interface, CRC Press; 1st edition (November 29, 1999), ISBN-13: 978-0849302664